Dear Referee #1
Thank you for thoroughly reading and commenting the manuscript. Please find below the replies to your suggestions; each of your suggestions is followed by the corresponding reply in bold letters and (where appropriate) actions taken to address it in the updated version of the manuscript in italics.

Comments:

The manuscript "Multi-species inversion and IAGOS airborne data for a better constraint of continental scale fluxes" by Boschetti et al. describes the effect of including the correlations between multiple species in a bayesian inversion framework in order to improve error reduction compared to solving for individual species independently. The experiment described in the manuscript uses synthetic observations based on measurements made during the IAGOS campaign in Europe in order to assess the potential for future measurements of CO_2, CO and CH_4 during this campaign to better constrain regional emissions of all three species. Finally, there is some discussion of the effect of different assumptions about the prior error of the emissions upon the level of error reduction achieved by the inversion.
Overall the manuscript is fairly well written, with few technical corrections necessary. The figures are generally quite clear and well chosen, although some further detail needs to be provided for some of them. The methods and models used within the manuscript are appropriate for such a study, and are able to provide some assessment of the potential for improvement supplied by future multi-species measurements as part of the measurement campaign. The paper is successful as far as it goes, and whilst it would have been nice to further examine the effect of different experiment set-ups within this paper, the authors acknowledge that this is the case, and may be the focus of a future manuscript.

We appreciate these positive remarks.

My main reservation with the study is that the results and discussion section is a little light on detail in places and feels like it was rushed, making the thread of the paper more difficult to follow than it should be. More details and deeper analysis of the results is needed in order to contextualize the findings of the experiment. The authors must make sure that all terms used have been explained or defined, and that they provide enough analysis of their results. See general comments for details. I suggest that this paper is suitable for publication in this journal after the following revisions are carried out and the results section is improved.

Thank you for the constructive comments. In the revised version …

Page 3 line 6: "Because most biogenic fluxes in Europe are influenced by human activities..." - reference?
We have added references and modified the sentence to:

"Because most biogenic fluxes in Europe are influenced by human activities, with 22% of Europe's land is dedicated to agriculture (FAO, 2013) and 45 % covered by forests, of which 80% are managed for wood supply (UNECE, FAO, 2011), understanding and managing these biogenic fluxes must also be a component of any policy to reduce anthropogenic emissions."

Page 4, lines 1-2: "proven to be important in the fields of..." - reference?
Two references were added; one for IAGOS and one for CONTRAIL (Zbinden et al, 2013; Sawa et al., 2012)

Page 8, line 18: the first term in equation (3) should be to the power of (-1).
The equation (3) was corrected accordingly

Page 8, line 31: the term "50% footprint" should be explained.
A reference to section 2.1.2 was added to remind the reader of the 'footprint'; the section now reads:
"As a spatial aggregation scale we chose an area from which fluxes have a significant contribution to the observations made at Frankfurt. For this we compute the temporally accumulated footprint values for the whole year 2011, and select those spatial pixels that correspond to 50% of the total (spatially integrated) footprint (Fig. 1)."

We also modified Section 2.1.2 (Pag. 6, Line 12) to better explain the concept of footprint:
"...so-called "footprints". Briefly, for each measurement location and time (also called receptor point), the model releases an ensemble of virtual particles that are driven back in time using simulated wind fields from ECMWF and turbulence as stochastic process; the residence time within the lower half of the mixed layer is used to determine the potential contribution from surface fluxes, and the cumulative sum of these contributions determines the footprint, that identifies the part of the domain with a certain influence on a single receptor point. This footprint is then matrix-multiplied with an emission map to derive the corresponding simulated mixing ratio in a given receptor point."

Page 8, line 15: is it fair to assume no correlation between months? You should comment here (or later in the discussion) on whether this would be the best set-up of the correlation matrix in an inversion using real observational data.
In page 10, line 16, the following was added:
In this study, we assume a certain annual total domain wide flux uncertainty, and then break it down by sectors, fuels, and months by inflating the error. By assuming no correlation between different months we ensure maximum flexibility in the system to retrieve month-to-month changes based on the observations. Assuming correlation between months would be possible, but has not been investigated here. It is unclear how good the seasonal variation in emissions from the inventories actually is, so in order to not rely too much on these we chose zero correlation.

Investigating the effects of different correlation set-ups for the seasonal cycle could be the focus of future research.

Page 12, line 4: What is *enh*?

Right after equation (11), the line *"…where enh indicates the modelled enhancement, and both the horizontal …"* **was added for clarity**

Page 12, line 7-8: You need to explain how you derive ε␣ tran_v in more detail here.

The text (from Page 12, line 6) was edited as follows:

… where both the horizontal transport error ε_{tran_h} and the vertical transport error ε_{tran_v} are characterized as percentage error; ε_{tran_h} is assumed to be 50% while ε_{tran_v} is profile-specific with mean value about 10%.

"The vertical transport error accounts for the fact that the shallower the mixed layer is, the more difficult it is to model the atmosphere. We assume that after zi-correction the remaining error is on the order of 50 m (related to the vertical resolution of the profile data), so the relative error ε_{tran_v} is assumed as the ratio of 50 m to the modeled z_i; in this way we obtain an error that gets larger the shallower the mixed layer is. "

Page 12, line 18: What method do you use to invert **Sprior** and **Se** ?

We assume this comment refers to Pag 8, eq. (3) and (4). The error correlation matrices are inverted using the R-function "solve" of the base package. At pag. 8, line 26 the following was added:

In this study, the inverse of the matrix was calculated using the R-function 'solve' from the base package.

Page 13, line 5: Describe which version of the model output you are plotting in Figure 5. Does it use the prior emissions?

We edited the text at lines 3-4 as follows:

Figure 5 shows … for both observations and model outputs using prior emissions.

Page 13, line 9: Here, and in the caption of Figure 5, you say that the modelled CO is multiplied by a factor of 2.8. However, the legend of Figure 5 appears to say that the observations have been scaled. Which is correct?

The text and the caption were correct. The legend has been corrected accordingly

Page 13, line 12: Explain here what it is that is indicated by the performance of the model compared to the observations. Are you saying that the meteorology that you use and the correction to zi that you apply produce a good indication of the temporal variation of the ML enhancement? Does your choice of zi display an improvement over the original?

Thank you for pointing this out. We have now investigated the improvement brought about by using the zi correction. The text in line 10 and following were edited as follows:
"Mixing ratios are highly variable, but the model produces a good indication of the temporal variation of the ML enhancement; the squared correlation coefficient between observed and modeled CO enhancements is 0.62, while the standard deviation of corrected model and observation residuals is 85 ppb; note that by not accounting for the z_i *correction, such values would be 0.56 and 87 ppb respectively. The median of the mixing ratio enhancement for the three trace gases is 2.8 ppm for* CO_2*, 18.6 ppb for CO and 26.6 ppb for* CH_4*."*
-- Note: we found that in the uploaded version of the paper the zi correction was actually switched off. After switching the correction on, only Figure 5 is affected. The mean uncertainty reduction values are now 35% for CO2_ff, 48% for CO and CH4, 60% for GEE and 63% for respiration. We deeply apologize for the mistake --

Page 13, lines 25 and 26: You could probably add a little more detail to this one-sentence paragraph. Explain that Figure 6 is showing the prior and posterior emission error covariance matrices for the base multi-species inversion. Do the single-species matrices show a similar overall error reduction? Do you expect to see negative correlations in the posterior matrix? As it stands this sentence is disjointed and appears to come out of nowhere and doesn't relate to other text, making the manuscript unnecessarily difficult to follow.
We propose to replace the one-sentence paragraph with the following:
"Figure 6 shows the prior and posterior error covariance matrices for the base multi-species inversion. The posterior error covariance matrix for the multi-species inversion (Fig. 6b) shows lower values corresponding to an average uncertainty reduction of 23% across all state vector elements, while the posterior error covariance matrix for the single-species inversion (not shown) is characterized by a mean uncertainty reduction of 20%. This result implies that the multi-species inversion improves the uncertainty reduction by roughly 15%. Negative values in the posterior error correlation matrix are to be expected because different categories are bind together by correlations and therefore are not free to vary independently."

Page 14, lines 24 - 28: Explain what you mean by "a perturbed version of the prior" here. Also, does the multi-species inversion capture the "truth" any better or worse than the single-species inversion?
We propose to add the two following sentences at Line 25:
"Such perturbed version is obtained by adding realization of the prior error to the prior state space, similarly to how the "truth" is obtained. In addition, it was found that the truth-posterior bias of the multi-species inversion is mostly slightly lower compared to the single-species inversion. Such difference is between -2.2% and 7.5%, according to the simulated species, with an overall value of 0.3%."

Page 15, line 19: How robust do you think the relative uncertainty reductions

that you derive are against different manifestations of the "true" fluxes?
What we investigate in Fig. 10 is not the uncertainty reduction, but the benefit from a multi-species inversion over a single-species one.
The following text was added at line 19:
The benefit of including inter-species correlations shown in Fig. 10 does not depend on different manifestations of the true fluxes, but only on the posterior uncertainty of the multi- and single-species inversions.

Page 15, line 26: Why do you think a smaller prior error for the CO2 FF fluxes compared to the other species leads to a greater uncertainty reduction for the posterior fluxes?
What we investigate in Fig. 10 is not the uncertainty reduction, but the benefit from a multi-species inversion over a single-species one. Uncertainty reduction for CO2 FF is actually greater in Case 1 (36%) compared with the other two cases (29% and 21% respectively), as in those cases (2 and 3) the prior is assumed to be known better already.

We have stated in the paper (page 15, line 26) that the benefit from a multi-species over a single-species inversion increases, when changing the prior uncertainty for CO2 emissions. We think that the reason is the following: changing the prior uncertainty in CO2 emissions means changing also the off-diagonal blocks linking the different species together (see Eq. 8). However, the diagonal block for CO2 in the prior uncertainty changes by a factor four in that case, while the off-diagonal blocks change only by a factor of two. This effectively ties the emissions of CO2 tighter to the emissions of the other species, resulting in more benefit from a multi- over a single-species inversion. Note that this is related to the required rescaling of the prior error covariance matrix described in section 2.1.5.

We suggest adding the following text at line 28:
…for this increase in benefit. The reason for both of these results is probably to be searched in Eq. 8. In fact, changing the prior uncertainty in CO_2 emissions means to also change the off-diagonal blocks linking the different species together. However, by reducing the anthropogenic CO_2 uncertainty from 20% to 10% (Case 2), the diagonal block for CO_2 in the prior uncertainty changes by a factor four, while the off-diagonal blocks change only by a factor of two. This effectively ties the emissions of CO_2 tighter to the emissions of the other species, resulting in more benefit from a multi- over a single-species inversion. Conversely, when all prior uncertainties are reduced by a factor 2 (Case 3), both diagonal and off-diagonal blocks are reduced by a factor four. This explains why Case 1 and Case 3 show similar benefit values.

Page 16, line 3: What makes CO sensitive to different correlation structures during different seasons?
To explain the issue, we added a couple of sentences at line 4:
What makes CO sensitive to different correlation structures during different seasons is that CO enhancement shows a stronger seasonal cycle compared to e.g.

fossil fuel component of the CO_2 enhancement, with average values for January of around 150 ppb (25 ppm for CO_2), and for July of 9 ppb (4 ppm for CO_2). This results in a much weaker constraint on the CO emissions from the CO observations during summer, but still some constraint through the other species such as CO_2 via the a priori correlation in the emissions.

Technical corrections:

Page 1, line 13: no comma needed in "for, GEE"
The text was edited according to the suggestion

Page 1, lines 17 and 18: the percentages reported in the abstract here are in some cases slightly different to those reported in the main text of the manuscript (on page 15).
The percentage values were checked and replaced where needed

Page 2, line 2: difference -> differences
The text was edited according to the suggestion

Page 5, line 10: Matherial -> Material
The text was edited according to the suggestion

Page 10, line 3: Section 2.1.6 -> Section 2.1.5
The text was edited according to the suggestion

Page 16, line 18: Delete "meaning" - or explain what it means.
The word "meaning" was removed as suggested

Additional changes made to the manuscript on top of those mentioned in the official replies to the reviewers comments as posted in the discussion page:
As the synthetic data experiment relies on random numbers generated to create realizations of prior errors, accidentally a new random number was chosen to regenerate the tables and figures. This affected Figs. 7 and 8 as well as the new table 5 (introduced in reply to reviewers #2 and #3). Also for the initial generation of table 5 different realizations of the prior error were chosen to generate the true state vector, now a single realization was used consistently. In addition a small error in the calculation of the posterior uncertainties in table 5 was fixed.

Dear Referee #2

Thank you for thoroughly reading and commenting the manuscript. Please find below the replies to your suggestions; each of your suggestions is followed by the corresponding reply in bold letters and (where appropriate) actions taken to address it in the updated version of the manuscript in italics.

Major comments:

1. While I agree that inclusion of prior error correlations between different emissions can improve observation constraint, and help disentangle sources, improper characterization of the error correlation may result in systematic bias in the posterior estimate. So I suggest a more complicated OSSE is necessary, where perturbations are generated using different correlation parameters to exam how well the system will reproduce the 'true' fluxes, with incorrect correlation coefficients.

This is a very useful suggestion, which we followed now. We propose to add the following at Page 14, Line 29

"Improper characterization of the error correlation may result in systematic bias in the posterior estimate. As mentioned in Sect. 2.1.6, inter-species correlation, the correlation between different fuel types and the correlation between different emission sectors in $\boldsymbol{S_{prior}}$ *is assumed equal to 0.7 (Sect. 2.1.4). To assess how well the system will reproduce the 'true' fluxes with incorrectly specified correlations, a series of experiments was performed in which the inter-species correlation in* $\boldsymbol{S_{\varepsilon}}$ *remains equal to 0.7, while the three correlation coefficients in* $\boldsymbol{S_{prior}}$ *assume different values ranging from 0.1 to 0.9. Table 5 shows the residuals between total annual posterior fluxes and total annual true fluxes for the five simulated species, derived similarly as for Table 4. We found that for all species the uncertainty reduction increases with correlation. More precisely, from correlation 0.1 to 0.9, the annual uncertainty reduction for anthropogenic* CO_2 *increases from 26.6% to 51.7%, while the increase is lower for GEE (from 72.4% to 73.1%) and respiration (from 39.3% to 41.3%) because the biospheric fluxes are independent from other species. For CO, the uncertainty reduction increases from 60.7% (with correlation 0.1) to 66.4% (with correlation 0.9). The annual uncertainty reduction for* CH_4 *increases from 60.5% to 67.5%.*

In addition, the posterior-truth biases are always lower than the prior-truth biases. The posterior uncertainty values (1-sigma) are usually larger then the corresponding bias values as expected, except for CO and for CH_4 *with prior correlations equal to 0.9. Thus the posterior is not significantly different from the truth. Conversely, the prior (not shown) is significantly different from the prior in the majority of cases for fossil fuel fluxes, and in some cases also for biogenic fluxes. The effect of assuming the incorrect error correlations appears to be in general small, possibly implying a relative robustness of our methods. Following this result, the fact that* CH_4 *is only partially co-emitted with* CO_2 *and CO should not affect the inversion in a strong way. For all of the experiments, the residuals between true and posterior fluxes are lower than residuals between true and prior fluxes for each of the simulated species; the difference between the cases with maximum and minimum residuals is around 4.2%. In addition, we found that the posterior* *aggregated fluxes in the nine experiments are not significantly different from each other, implying that the system is fairly robust against errors in the assumed inter-species correlation."*

We also added a new table 5 in the revised manuscript:

Correlation	Post-Truth CO_2 ff	Post-Truth CO	Post-Truth CH_4	Post-Truth GEE	Post-Truth Respiration
0.1	-6.3 ±16.4	-0.3 ± 0.2	-0.1 ± 0.3	-18.5 ± 23.6	-19.0 ±27.5
0.2	-4-4 ±16.1	-0.3 ± 0.2	0.0 ± 0.3	-18.6 ± 23.5	-19.2 ±27.4
0.3	-2.7 ±15.9	-0.3 ± 0.2	0.0 ± 0.3	-18.6 ± 23.4	-19.5 ±27.3
0.4	-1.3 ±15.6	-0.3 ± 0.2	0.0 ± 0.3	-18.5 ± 23.4	-19.7 ±27.3
0.5	-0.1 ± 15.2	-0.3 ± 0.2	0.0 ± 0.2	-18.4 ± 23.3	-20.0 ±27.2
0.6	0.8 ± 14.6	0.3 ± 0.2	0.1 ± 0.2	-18.2 ± 23.2	-20.3 ±27.1
0.7	1.5 ± 13.7	-0.3 ± 0.2	0.1 ± 0.2	-17.9 ± 23.2	-20.6 ±26.9
0.8	1.9 ± 12.4	-0.3 ± 0.2	0.2 ± 0.2	-17.6 ± 23.1	-20.9 ±26.8
0.9	1.5 ± 10.4	-0.4 ± 0.2	0.3 ± 0.2	-17.3 ± 23.0	-21.1 ±26.5

Table 5: Residuals between total annual posterior fluxes and total annual true fluxes for the five simulated species (in MtC/yr) and different inter-species correlation values in the prior error covariance matrix (first column). The corresponding posterior uncertainty was added for each Post-Truth value.

-- Note to the Referee: the values for the correlation of 0.7 do not exactly reproduces the values in Table 4, as we realized that in the uploaded version of the paper, the zi-correction described in section 2.1.1 was mistakenly turned off. This has been fixed in the revised version, and the updated Table 4 has values matching the 7th row of Table 5.

For all of the experiments, the residuals between true and posterior fluxes are lower than residuals between true and prior fluxes for each of the simulated species; the difference between the cases with maximum and minimum residuals is around 4.2%. In addition, we found that the posterior aggregated fluxes in the nine experiments are not significantly different from each other, implying that the system is fairly robust against errors in the assumed inter-species correlation.

2. Discussions are more focused on the domain total. It is interesting to see how well the system will reproduce their spatial distribution.

1) Note that we do actually not focus on the domain total, as we believe it is not reasonable to constrain the whole European domain when pseudo-observations are focused only around a single city; for this reason we chose the region marked by the 50% footprint area, that contains most of the surface influence. We suggest to add the following sentence at page 8 – line 30:

As the pseudo-observations are clustered around a single location (Frankfurt), fluxes over the whole European domain can very likely not be constrained. Therefore, as spatial aggregation scale we chose a domain…

2) Regarding the reproduction of spatial distribution: Our modeling framework does not optimize the emissions in the individual grid-cells, but only the scaling factors for emissions from different sectors and fuel types. With this modeling framework it is not possible for us to evaluate how well the spatial distribution is reproduced.

Minor comments:

1. Line 5, Page 4: "This synergy follows from the fact . . ." Better changed to 'follows the fact. . .' or other phrase.

The text was edited according to the suggestion

2. Line 5, Page 14: ". . .have a magnitude of 6-11 Megatons of carbon per year (MtC y-1) in July" The unit of MtC/yr seems inconsistent with annual total presented in Table 5. I think it should be MtC/a.

In Table 4 (not 5), the total presented refers to overall residuals between (e.g.) total prior fluxes minus total true fluxes, aggregated over all emission categories. As such, they are not directly comparable with the amounts shown in Figure 7 (to which Line 5, Page 14 refers), which instead indicates the true fluxes for specific emission categories. Note that we chose to use the unit "MtC y^{-1}" over "MtC/a" as suggested by the journal 'Manuscript preparation guidelines for authors'.

3. Line 26, page 14: ".. .for the whole year between the prior and both posterior and the perturbed prior" The sentence is unclear.

The text was modified as follows:

"To do so, for each of the five simulated species we calculated the total annual fluxes for prior, posterior, truth, and perturbed prior. From these total fluxes we then derive the overall residual between prior and truth, posterior and truth, and perturbed prior and truth."

4. Figure 7: Please explain why for CH4 fluxes in December, their uncertainty has been significantly reduced, but the differences from the 'true' are not obviously improved.

It is normal for Bayesian inversion to have some elements of the posterior state space that are not obviously improved. The expectation is that the posterior values are in agreement with the true values within their respective uncertainty. As we use 1-sigma uncertainties, we expect about 36% to be even outside this uncertainty range. Note that the inversion for monthly fluxes solves for a total of 828 scaling factors for CH_4, of which about 70 contribute to 90% of the fluxes. However, the atmospheric signals associated with these 70 different sectors/fuel types are not observed directly, but only as a combined signal in CH_4.

5. Figure 6: I suggest the authors also provide the prior and posterior error correlation between CO2 fossil fuel emission and biospheric net flux in the main text.
A sentence was added to provide the correlations (Line 26, page 26)
Note that CO_2 from anthropogenic emissions is assumed to be independent from biogenic emissions; therefore prior error correlation between these categories is zero.

6. Figure 7: check the units for monthly fluxes (in main text as well).
The units in Figure 7 and 8 were changed to MtC/m. References to these figures in the main text were also given with this unit.

Additional changes made to the manuscript on top of those mentioned in the official replies to the reviewers comments as posted in the discussion page:
As the synthetic data experiment relies on random numbers generated to create realizations of prior errors, accidentally a new random number was chosen to regenerate the tables and figures. This affected Figs. 7 and 8 as well as the new table 5. Also for the initial generation of table 5 different realizations of the prior error were chosen to generate the true state vector, now a single realization was used consistently. In addition a small error in the calculation of the posterior uncertainties in table 5 was fixed.

Dear Referee #3
Thank you for thoroughly reading and commenting the manuscript. Please find below the replies to your suggestions; each of your suggestions is followed by the corresponding reply in bold letters and (where appropriate) the actions taken to address it in the updated version of the manuscript in italics.

General comments:

The paper presents a multi-species inversion framework tested using pseudo-data experiments. Various assumptions are made to evaluate the sensitivity of the inversion, with an emphasis on the impact of error correlations across species and sectors. Overall, the paper presents an innovative approach to assimilate various atmospheric species in a single inversion framework. This study is clearly worthwhile publishing but lacks a better evaluation of the aggregation operator assumption (perfect prior emission distribution) and the impact of systematic errors in the system affecting the correlations in the gas-sector attribution problem. The Observing System Simulation Experiments (OSSE's) cover some of the assumptions with varying levels of uncertainties but several components are not carefully considered. The two major concerns here are the aggregation operator, that remains perfectly known and so the spatial distribution of the prior fluxes, and the assessment of correlations among sectors and across trace gases for the different species that remain very unclear. A last but less critical concern is related to the assumption that transport errors are similar across species, which is unlikely for CH_4 and CO_2 for example, rarely co-emitted (only CO_2-CO is discussed) and therefore affected by different problems in different parts of the domain. The work focuses primarily on random errors and ignores systematic errors that remain the main limitations in atmospheric inversions. Therefore, this study requires some additional experiments before publication, specifically addressing the error associated with the aggregation operator and errors in gas ratios for the different sectors.

- The use of an aggregation operator needs to be discussed. Hyper-parameters (here scaling factors for the sectors) are used to reduce the dimension of the problem but correspond to an assumption of perfectly-known distributions. The system should be evaluated not only under the "perfect spatial distribution" assumption, especially for CO_2 biogenic fluxes which are clearly not well-known. One suggestion to clarify the concern here would be to use VPRM as truth but assumes a different distribution when constructing the aggregated solution such as the posterior fluxes from Panagiotis et al. (2016). Other experiments could be designed here to test the aggregation problem. Similarly, the area defined by half of the total footprint is arbitrary and never tested nor justified. Why 50% was used? How much variations are expected within that area which would affect the error correlations? If a power plant is located near an airport, how would that affect the CO/CO_2 correlations and therefore the homogeneity within the aggregated area?

Note that we do actually not focus on the domain total, as we believe it is not reasonable to constrain the whole European domain when pseudo-observations are focused only around a single city; for this reason we chose the region marked by the 50% footprint area, that contains most of the surface influence. We suggest to add the following sentence at page 8 – line 30:
… into physically representative quantities. As the pseudo-observations are clustered around a single location (Frankfurt), fluxes over the whole European domain can very likely not be constrained. Therefore, as spatial aggregation scale we chose a domain…

To the main point of this comment, we actually do not exactly assume perfect knowledge of the spatial distribution of total emissions; it is only within each sector and fuel type the spatial pattern of the emissions are assumed to be known.

We admit that the modeling framework that we set up is not particularly well suited to investigate the aggregation error. However, the chosen domain is quite small, and the total fossil fuel fluxes are divided according to species, emission categories, fuel types and months. This result in numerous degrees of freedom available to resolve biosphere fluxes, and for this reason we expect the aggregation error not to be a particularly important source of uncertainty.

In our inversion, as in all inversions, the near field is a critical domain in the arising of systematic errors. The better way to address systematic errors is of course by comparing model outputs with real observations, which are currently unavailable. The bias errors in atmospheric inversions making use of airborne measurements will have to be addressed anyway, once real observations from IAGOS will be available. For this reason, in this paper we chose to focus on random errors instead.

We suggest to add the following sentence at page 8 – line 31:
… 2011 (Fig. 1). Note that by using this aggregation scale we assume perfectly-known distribution within a given flux category that can result in aggregation error, especially with respect to biogenic fluxes, that are not so well known as anthropogenic fluxes. However, the chosen domain of aggregation is quite small, and the total anthropogenic fluxes are divided according to species, emission categories, fuel types and months. This result in 69 numerous degrees of freedom per month for each anthropogenic species and 10 degrees of freedom per month for the biospheric fluxes; for this reason we expect the aggregation error not to be a particularly important source of uncertainty.

- The discussion about error correlations across species is confusing. How did you define the emissions for the different sectors? Have you assigned gas ratios to various sectors? If so, what are these ratios? Some of the discussions are related to using CO2 and CO data to diagnose gas-to-gas correlations, but the exact definition of the emissions of the different gases for each sector has been defined in the inversion system. Or maybe the sectors are unrelated for each gas? The different sectors have ratios in terms of trace gas emissions but these emission ratios vary regionally. This section needs to be explained in more details. The assumptions made here should also be tested in the inversion framework.

Emission ratios are not used here, but we used instead bottom-up calculated emissions for each of the three gases, using different emission sector-specific factors, which are for CO also region-specific. These country emissions are then gridded consistently with geospatial proxy data that are representative for the emitting activity, common to all species for the multi-species sources.

We suggest the following changes to the text:

Add at page 7, line 1:
...on our regional European domain. For each of the three anthropogenic modeled species (CO_2, CO and CH_4), different emission maps are used as input. Temporal profiles are then applied to these sector- and fuel-specific emission maps.

Replace at page 14, from line 5 to line 24:
CO2 and CO are dominated by combustion sectors (Fig. 8). The most important emission sectors for CO2 are energy, industry, transport and building, each contributing 7-10 MtC y-1 in July and 6-14 MtC y-1 in December. Dominant fuels (Fig. 7) for CO2 are coal, gas and oil, whose prior fluxes (pseudo data) have a magnitude of 6-11 Megatons of carbon per year (MtC y-1) in July and 8-14 MtC y-1 in December. For CO the most important emission sector is heating of buildings during winter contributing a 0.19 MtC y-1 flux with only secondary contributions from industry and transport with a magnitude of 0.04 MtC y-1 and 0.05 MtC y-1 respectively (during July and December). The dominant fuel for CO is biofuel with 0.19 MtC y-1 emissions during winter. The secondary industrial and transport contributions originate in summer from oil and biofuels with a magnitude of 0.06-0.08 MtC y-1 and from agricultural waste burning with a magnitude of 0.06-0.11 MtC y-1.

Contrary to CO2 and CO, CH4 is determined by non-combustion sectors, more specifically by a contribution of 0.15 MtC y-1 flux from agriculture (manure management and rice cultivation) in July with secondary contributions from waste and energy with a magnitude of roughly 0.06-0.08 MtC y-1 in both July and December. Other non-combustion sectors, in particular wastewater treatment and landfills contribute to a total of 0.16-0.24 MtC y-1 of emissions. These non-combustion sectors contribute to less than 20% of total CO2 emissions, with 1.13 MtC y-1 from the cement and lime industry and less than 20% to the total CO emissions (0.03 MtC y-1 from the metal industry).
The contribution to CO_2 from biospheric primary production (a sink for atmospheric CO_2) is about 100 MtC y-1 in July, which drops to almost zero in

December, while respiration values are 50 MtC y-1 in July and roughly 150 MtC y-1 in December.

- CO biogenic fluxes: the paper does not address the problem of CO biogenic fluxes during the growing season. Warm days in summer correspond to large amount of biogenic VOC's being emitted from the vegetation, producing CO to non-negligible levels. This issue should be discussed if not addressed. How would this problem affect the ability to retrieve the truth?

To discuss this issue we propose to add the following at page 14, line 4:

Note that our modeling framework does not allow for simulating CO biogenic fluxes during the growing season. Warm days in summer correspond to large amount of biogenic VOC's being emitted from the vegetation, producing CO to non-negligible levels. According to Hudman (2008), anthropogenic emissions accounts for only 31% of CO emissions in the US during summer. Conversely, according to estimates from EDGAR, CO anthropogenic emissions during summer are about 18% of the annual anthropogenic emissions. Combining these two results, one could conclude that CO production from biogenic sources accounts for roughly 42% of total annual CO emissions.

In general, the absence of some emission sources in an inventory is equivalent to the assumption of having point sources not included in the emission map, but still contributing to the measurements. The inversion scheme would typically react to this by assigning such point sources in some other sector other fuel type. As a result, the posterior enhancements would be biased low in proximity of that point sources, and (slightly) biased high for influences from other regions with the same sector or fuel type. This issue should definitely be considered in a future study making use of actual CO, CO_2 and CH_4 observations from IAGOS but has limited effects on this paper, as our main focus is on the benefits of inter-species correlation on the posterior uncertainty in the frame of a synthetic experiment.

- When you constructed your error correlations for CH4, transport errors are unlikely to be highly correlated as CH4 is only partially co-emitted with CO2 and CO. Large emissions from NG production and farming activities are uncorrelated with biogenic or fossil fuel consumption. This problem should be addressed here. If transport errors, which are spatially variable, affect CH4 and CO2/CO in different ways, the error correlation would be affected. Additional experiments using incorrect error correlations would quantify the sensitivity of the inverse fluxes to the assumptions made in prior errors.

This is a very useful suggestion, which we followed now. We propose to add the following at Page 14, Line 29

"Improper characterization of the error correlation may result in systematic bias in the posterior estimate. As mentioned in Sect. 2.1.6, inter-species correlation, the correlation between different fuel types and the correlation between different emission sectors in $\mathbf{S}_{prior}$ is assumed equal to 0.7 (Sect. 2.1.4). To assess how well the system will reproduce the 'true' fluxes with incorrectly specified correlations, a series of experiments was performed in which the inter-species correlation in $\mathbf{S}_{\varepsilon}$

*remains equal to 0.7, while the three correlation coefficients in **S_{prior}** assume different values ranging from 0.1 to 0.9. Table 5 shows the residuals between total annual posterior fluxes and total annual true fluxes for the five simulated species, derived similarly as for Table 4. We found that for all species the uncertainty reduction increases with correlation. More precisely, from correlation 0.1 to 0.9, the annual uncertainty reduction for anthropogenic CO_2 increases from 26.6% to 51.7%, while the increase is lower for GEE (from 72.4% to 73.1%) and respiration (from 39.3% to 41.3%) because the biospheric fluxes are independent from other species. For CO, the uncertainty reduction increases from 60.7% (with correlation 0.1) to 66.4% (with correlation 0.9). The annual uncertainty reduction for CH_4 increases from 60.5% to 67.5%.*

In addition, the posterior-truth biases are always lower than the prior-truth biases. The posterior uncertainty values (1-sigma) are usually larger then the corresponding bias values as expected, except for CO and for CH_4 with prior correlations equal to 0.9. Thus the posterior is not significantly different from the truth. Conversely, the prior (not shown) is significantly different from the prior in the majority of cases for fossil fuel fluxes, and in some cases also for biogenic fluxes. The effect of assuming the incorrect error correlations appears to be in general small, possibly implying a relative robustness of our methods. Following this result, the fact that CH_4 is only partially co-emitted with CO_2 and CO should not affect the inversion in a strong way. For all of the experiments, the residuals between true and posterior fluxes are lower than residuals between true and prior fluxes for each of the simulated species; the difference between the cases with maximum and minimum residuals is around 4.2%. In addition, we found that the posterior aggregated fluxes in the nine experiments are not significantly different from each other, implying that the system is fairly robust against errors in the assumed inter-species correlation."

We also added a new table 5 in the revised manuscript:

Correlation	Post-Truth CO_2 ff	Post-Truth CO	Post-Truth CH_4	Post-Truth GEE	Post-Truth Respiration
0.1	-6.3 ±16.4	-0.3 ± 0.2	-0.1 ± 0.3	-18.5 ± 23.6	-19.0 ±27.5
0.2	-4-4 ±16.1	-0.3 ± 0.2	0.0 ± 0.3	-18.6 ± 23.5	-19.2 ±27.4
0.3	-2.7 ±15.9	-0.3 ± 0.2	0.0 ± 0.3	-18.6 ± 23.4	-19.5 ±27.3
0.4	-1.3 ±15.6	-0.3 ± 0.2	0.0 ± 0.3	-18.5 ± 23.4	-19.7 ±27.3
0.5	-0.1 ± 15.2	-0.3 ± 0.2	0.0 ± 0.2	-18.4 ± 23.3	-20.0 ±27.2
0.6	0.8 ± 14.6	0.3 ± 0.2	0.1 ± 0.2	-18.2 ± 23.2	-20.3 ±27.1
0.7	1.5 ± 13.7	-0.3 ± 0.2	0.1 ± 0.2	-17.9 ± 23.2	-20.6 ±26.9
0.8	1.9 ± 12.4	-0.3 ± 0.2	0.2 ± 0.2	-17.6 ± 23.1	-20.9 ±26.8
0.9	1.5 ± 10.4	-0.4 ± 0.2	0.3 ± 0.2	-17.3 ± 23.0	-21.1 ±26.5

Table 5: Residuals between total annual posterior fluxes and total annual true fluxes for the five simulated species (in MtC y^{-1}) and different inter-species correlation values in the prior error covariance matrix (first column). The corresponding posterior uncertainty was added for each Post-Truth value.

- The problem of unreported sources in CH4 inventory is not addressed at all. Recent papers have discussed the lack of information for natural gas and oil production operations, or from recent and old mining areas. How would unreported sources affect the inverse solutions? This question comes back to the aggregation operator.

To discuss this issue we propose to add the following at page 14, line 4:

Our modeling framework is currently not well suited to account for unreported sources of CH_4 due to the lack of information about natural gas and oil production operations, or from recent and old mining areas.. Many recent studies have discussed the problem, mainly referring to shale basins exploited via hydraulic fracturing in the US (e.g. Kort et al., 2016; Karion et. al, 2015; Lyon et al., 2015). For example, Karion (2015) concludes that EDGAR underestimates methane emissions associated with oil and gas industry by a factor of 5 in the US.

However, the situation over the European continent may be quite different. In a review about risk assessment of shale gas development in the UK, Prpich (2015) reports that the European Union is generally much more cautious about unconventional oil and gas sources, while a recent study on a methane plume over the North Sea (Cain et al., 2017) concluded that the bulk signature of said plume originated from on-shore coal mines and power stations in the Yorkshire area.

In general, the absence of some emission sources in an inventory is equivalent to the assumption of having point sources not included in the emission map, but still contributing to the measurements. The inversion scheme would typically react to this by assigning such point sources in some other sector other fuel type. As a result, the posterior enhancements would be biased low in proximity of that point sources, and (slightly) biased high for influences from other regions with the same sector or fuel type. This issue should definitely be considered in a future study making use of actual CO, CO_2 and CH_4 observations from IAGOS but has limited effects on this paper, as our main focus is on the benefits of inter-species correlation on the posterior uncertainty in the frame of a synthetic experiment

- The utility of the figures showing the multiple error covariance matrices for the different cases remains limited. The information content would be better described with words or mathematically. Readers cannot extract useful information from contour plots of covariance matrices. They could remain part of the paper but as part of the supplementary information. A table could also synthesize the various assumptions tested in the inversion system.

We propose to add axis label to Fig. 2,3,4 to increase readability. Such axis should identify different species, emission sectors, fuel types and vegetation categories.

Technical comments:

3-1: Consequently, intercomparisons...
The text was edited according to the suggestion

3-3: the international level
The text was edited according to the suggestion

3- 1st paragraph: This paragraph is confusing and not always following a logical path. Prediction skills and emission reduction are two different problems not directly connected to each other. Explain better the broad context of this study by focusing on the main general issues and clarify which one you are trying to address here.
The paragraph was rephrased as follows:
As widely recognized at the international level, there is a need for reduction in anthropogenic emissions (IPCC). This however implies the necessity for reliable climate predictions from atmospheric models in order to allow policymakers to take informed decisions. Unfortunately, current climate predictions are hampered by excessive uncertainties; for example intercomparisons of different models show important differences on their predictions as shown in Friedlingstein (2016). This makes it difficult to assess the better environmental policies to implement. Because most biogenic fluxes ...

3-10: A commonly used approach to estimate...
The text was edited according to the suggestion

3-13: Actually, the uncertainty reduction relies purely on the assumptions made in the system and not on the effective ability of the system to produce a reliable solution. Bayesian system assumes that data will improve the a priori by construction. Explain better what you mean here.
The text was modified as follows.
As the main goal of this study is to assess the benefit of inter-species correlations in reducing the uncertainty of the posterior state space, we are particularly interested in the effects of such correlations on the uncertainty reduction, defined as the difference between prior and posterior uncertainty normalized by the prior.

3- 2nd paragraph: Several papers are missing here. For example, CO2-CH4 inversion using satellite data (Pandey et al., 2015) or the optimization of co-emitted species (Brioude et al., 2012), and early work on delta 13-CO2 by Enting et al. (1995). The authors should dig into atmospheric chemistry studies where several studies have addressed the use of multiple co-emitted species to constrain emissions at small scales.
Previous studies using multiple species to constrain emissions should be

introduced here, even without having used a formal inversion framework, such as urban studies over Los Angeles (e.g. Peischl et al., 2013). The optimization problem is equivalent and relies on similar ideas to constrain the emissions.

We replaced the text at Pag. 3, lines 20-22 with:

Several studies have made use the correlations among different species. One of the first example is the work from Enting (1995) on CO_2 and $^{13}CO_2$, while Brioude (2012) attempted to derive a CO_2 emission inventory without a prior emission estimate, instead using inventories of CO, NO_y and SO_2. Similarly, Peischl (2013) made use of CO and CO_2 inventories to help quantifying sources of CH_4 in the Los Angeles basin. The ability of measuring multiple species has been proved useful also in remote sensing. For example, Pandey (2015) made use of simultaneously retrieved CO_2 and CH_4 total column to reduce scattering effect. Further examples of studies making use of co-emitted species can be found in the frame of atmospheric chemistry (Konovalov et al., 2014; Berezin et al., 2013; Pison et al., 2009). More focused on exploiting inter-species correlation to reduce uncertainty in the frame of Bayesian Inversion, Palmer (2006) made use of CO2-CO correlations to improve an inversion using data from the TRACE-P aircraft mission, while Wang (2009) employed a similar method using satellite data, obtaining a reduction in the flux error of a CO_2 inversion.

5-24: This technique assumes that the wind direction and speed are comparable near the surface and at 2km high. Mass-balance studies have shown that this is often not the case (e.g. Karion et al., 2015). Free troposheric air represents different air masses due to the wind direction and speed gradients in the vertical. This assumption would need to be tested with the particle model.

This is a misunderstanding. We do not rely on winds within the mixed layer and the wind above to be comparable, as our transport operator H represents the mixed layer enhancements appropriately. We added the following text to

... a single footprint is derived. To represent the mixed layer enhancements, the footprints for receptors within the boundary layer are averaged, and the footprint for the free tropospheric receptor is subtrated from this, resulting in a footprint for the mixed layer enhancements. This footprint is then matrix-multiplied ...

7-3: What about CO biogenic fluxes? During warm summer times, biogenic CO fluxes represent a significant fraction of the signals. Did you ignore this contribution in your study?

A similar comment has already been addressed (see above).

2.1.3 To reduce the dimension of the state vector, you assume here that the spatial distribution of the prior fluxes and emissions are perfect, using an aggregation operator. This approach is reasonable for fossil fuel emissions but less convincing for biogenic fluxes.

A similar comment has already been addressed (see above).

12-28: How did you take into account the truncation of the prior errors? Did you adjust the truncated random perturbations to match the non-truncated assumption made in the prior error covariance matrix?

The error realization is obtained by multiplying a randomly generated, normally distributed vector with the prior error covariance matrix. This ensures that such realization has the same error correlation of the prior uncertainty. Where the result of such matrix-vector product is negative, the same operation is performed recursively until all elements of the state vector are positive. We suggest adding the following text at page 12 line 24:

… to avoid negative state vector values. In detail, the error realization is obtained by multiplying a randomly generated, normally distributed vector with the prior error covariance matrix. This ensures that such realization has the same error correlation of the prior uncertainty. Where the result of such matrix-vector product is negative, the same operation is performed recursively until all elements of the state vector are positive. This ensures that the difference …

Additional changes made to the manuscript on top of those mentioned in the official replies to the reviewers comments as posted in the discussion page:

As the synthetic data experiment relies on random numbers generated to create realizations of prior errors, accidentally a new random number was chosen to regenerate the tables and figures. This affected Figs. 7 and 8 as well as the new table 5. Also for the initial generation of table 5 different realizations of the prior error were chosen to generate the true state vector, now a single realization was used consistently. In addition a small error in the calculation of the posterior uncertainties in table 5 was fixed.

Multi-species inversion and IAGOS airborne data for a better constraint of continental scale fluxes

Fabio Boschetti[1],Valerie Thouret[2], Greet Janssens Maenhout[3], Kai Uwe Totsche[4], Julia Marshall[1], Christoph Gerbig[1]

[1]Max Plank Institute for Biogeochemistry, Jena, 07745, Germany
[2]Laboratoire d'Aerologie, CNRS and Universite' Paul Sabatier, Toulouse, 31400, France
[3]European Commission Joint Research Centre, Institute for Environment and Sustainability, Ispra, 21027, Italy
[4]Friedrich Schiller University, Jena, 07743, Germany

Correspondence to: Fabio Boschetti (fabosk@bgc-jena.mpg.de)

Abstract. Airborne measurements of CO_2, CO, and CH_4 proposed in the context of IAGOS (In-service Aircraft for a Global Observing System) will provide profiles from take-off and landing of airliners in the vicinity of major metropolitan areas useful for constraining sources and sinks. A proposed improvement of the top-down method to constrain sources and sinks is the use of a multispecies inversion. Different species such as CO_2 and CO have partially overlapping emission patterns for given fuel-combustion related sectors, and thus share part of the uncertainties, both related to the a priori knowledge of emissions, and to model-data mismatch error. We use a regional modeling framework consisting of the Lagrangian particle dispersion model STILT (Stochastic Time-Inverted Lagrangian Transport), combined with high resolution (10 km x 10 km) EDGARv4.3 (Emission Database for Global Atmospheric Research) emission inventory, differentiated by emission sector and fuel type for CO_2, CO, and CH_4, and combined with the VPRM (Vegetation Photosynthesis and Respiration Model) for biospheric fluxes of CO_2. Applying the modeling framework to synthetic IAGOS profile observations, we evaluate the benefits of using correlations between different species' uncertainties on the performance of the atmospheric inversion. The available IAGOS CO observations are used to validate the modeling framework. Prior uncertainty values are conservatively assumed to be 20%, for CO_2 and 50% for CO and CH_4, while those for GEE (Gross Ecosystem Exchange) and respiration are derived from existing literature. Uncertainty reduction for different species is evaluated on a domain encircling 50% of the profile observations' surface influence over Europe. We found that our modeling framework reproduces the CO observations with an average correlation of 0.56, but simulates lower mixing ratios by a factor 2.8, reflecting a low bias in the emission inventory. Mean uncertainty reduction achieved for CO_2 fossil fuel emissions is roughly 38%; for photosynthesis and respiration flux it is 41% and 44%, respectively. For CO and CH_4 the uncertainty reduction is roughly 63% and 67%, respectively. Considering correlation between different species, posterior uncertainty can be reduced by up to 23%; such reduction depends on the assumed error structure of the prior and on the considered timeframe. The study suggests a significant uncertainty constraint on regional emissions using multi-species inversions of IAGOS in situ observations.

Christoph Gerbig 18.12.17 16:05
Gelöscht: ,

Christoph Gerbig 18.12.17 16:05
Gelöscht: 37

Christoph Gerbig 18.12.17 17:25
Gelöscht: 5

1. Introduction

As widely recognized at the international level, there is a need for reduction in anthropogenic emissions (IPCC). This however implies the necessity for reliable climate predictions from atmospheric models in order to allow policymakers to take informed decisions. Unfortunately, current climate predictions are hampered by excessive uncertainties; for example intercomparisons of different models show important differences on their predictions as shown in Friedlingstein (2016). This makes it difficult to assess the better environmental policies to implement. Because most biogenic fluxes in Europe are influenced by human activities, with 22% of Europe's land is dedicated to agriculture (FAO, 2013) and 45 % covered by forests, of which 80% are managed for wood supply (UNECE, FAO, 2011), understanding and managing these biogenic fluxes must also be a component of any policy to reduce anthropogenic emissions.

A commonly used approach to estimate carbon budgets by teasing apart sources and sinks in a given spatial domain is the atmospheric Bayesian inversion. Atmospheric inversions combine prior knowledge from emission inventories with atmospheric observations acting as a top-down constraint to produce better posterior knowledge. As the main goal of this study is to assess the benefit of inter-species correlations in reducing the uncertainty of the posterior state space, we are particularly interested in the effects of such correlations on the uncertainty reduction, defined as the difference between prior and posterior uncertainty normalized by the prior. The vast majority of published papers on atmospheric inversions investigate the budget of a single species, usually a long-lived greenhouse gas like CO_2 (e.g. Rödenbeck, 2003) or CH_4 (e.g. Hein, 1997; Bousquet, 2006), but the technique can also be applied to active species like CO (Bergamaschi, 2000). Note that carbon dioxide is a special case as atmospheric CO_2 mixing ratios result from a combination of strong anthropogenic sources with strong sources and sinks from biospheric processes, calling for a separation of anthropogenic from biospheric fluxes. One way to achieve such a separation is to measure CO alongside CO_2, and use CO as a proxy for CO_2 anthropogenic emissions. Several studies have made use the correlations among different species. One of the first example is the work from Enting (1995) on CO_2 and $^{13}CO_2$, while Brioude (2012) attempted to derive a CO_2 emission inventory without a prior emission estimate, instead using inventories of CO, NO_y and SO_2. Similarly, Peischl (2013) made use of CO and CO_2 inventories to help quantifying sources of CH_4 in the Los Angeles basin. The ability of measuring multiple species has been proved useful also in remote sensing. For example, Pandey (2015) made use of simultaneously retrieved CO_2 and CH_4 total column to reduce scattering effect. Further examples of studies making use of co-emitted species can be found in the frame of atmospheric chemistry (Konovalov et al., 2014; Berezin et al., 2013; Pison et al., 2009). More focused on exploiting inter-species correlation to reduce uncertainty in the frame of Bayesian Inversion, Palmer (2006) made use of CO2-CO correlations to improve an inversion using data from the TRACE-P aircraft mission, while Wang (2009) employed a similar method using satellite data, obtaining a reduction in the flux error of a CO_2 inversion.

Christoph Gerbig 19.12.17 13:33
Gelöscht: Climate predictions are currently hampered by excessive uncertainties. A symptom of this is that intercomparisons of different models show important difference in their predictions, as shown in Friedlingstein (2006). This makes it difficult to assess the better environmental policies to implement. As is widely recognized at an international level, there is a need for the reduction in anthropogenic emissions (IPCC, 2014). This however implies the necessity for emissions monitoring to verify whether emission-reduction policies are successful.

Christoph Gerbig 19.12.17 13:38
Gelöscht: An important tool

Christoph Gerbig 19.12.17 13:39
Gelöscht: An important metric to measure the effectiveness of an atmospheric inversion is the uncertainty reduction, defined as the difference between prior and posterior uncertainty normalized with the prior uncertainty.

Christoph Gerbig 19.12.17 13:50
Gelöscht: Palmer (2006) used CO_2-CO correlations to improve an inversion of data from the TRACE-P aircraft mission in March-April 2001, while Wang (2009) employed a similar method using satellite data, obtaining a reduction in CO_2 flux inversion error.

So far the lion's share of the studies investigating atmospheric inversions make use of both continuous in situ and flask measurements from ground based observational networks of tall towers (e.g. Kadygrov, 2015; Sasakawa, 2010). However, as profiles collected from an aircraft easily exceed the height of towers, airborne data may also prove an interesting option for this application. This alternative was tested in some recent studies that made use of aircraft profiles alone or in combination with other data sources (e.g.: Brioude, 2013; Gourdji, 2013). Methods to maximise the cost-effectiveness of airborne data are the use of unmanned aircraft (drones) and commercial airliners. The latter, in particular, allows for collecting data on a regular basis without requiring a particularly small or light sensor. The most important projects making use of commercial airliners are CONTRAIL (Comprehensive Observation Network for Trace Gases) (Machida, 2008), and MOZAIC/IAGOS (Measurements of Ozone and water vapor by in-service AIrbus aircraft / In-service Aircraft for a Global Observing System) (Marenco, 1998; Petzold, 2015). Both projects have been running for more than two decades and have produced extensive datasets that have proven to be important in the fields of atmospheric modeling and satellite calibration and validation (Zbinden et al.,2013; Sawa et al., 2012). Regarding carbonaceous species, CONTRAIL has so far been collecting CO_2 mixing ratio measurement, while IAGOS was focused on CO. In the next years the IAGOS fleet will simultaneously provide CO, CO_2 and CH_4 atmospheric concentration measurements (Filges, 2015), enabling the use of multi-species synergy in modeling applications. This synergy follows the fact that the collocated measurements share the same atmospheric transport and have partially correlated emission uncertainties.

This paper is focused on investigating the benefits on uncertainty reduction of such a multi-species inversion in comparison with a single-species inversion. To attain this goal, we set up a synthetic experiment utilizing the measurement times and locations collected from the IAGOS projects in the year 2011. The present paper is intended to pave the way for future studies making use of multi-species IAGOS datasets when they become available. A receptor-oriented framework was set up to derive flux interactions between the atmosphere and the biosphere using IAGOS data. The modeling framework is composed of a Lagrangian Particle Dispersion Model (LPDM, specifically the STILT model), a diagnostic biosphere-atmosphere exchange model (the VPRM model), gridded emission inventories, global tracer transport model output that provides the tracer boundary conditions for the regional domain, and a Bayesian inversion scheme. The present work is based on the modeling framework used in Boschetti (2015) and builds upon that by adding other species, and using a formal Bayesian inversion. A multi-species inversion was carried out in order to exploit the correlations in uncertainties between CO_2, CO, and CH_4, specifically in their respective uncertainties in a priori anthropogenic emissions and in model representation error. The aim of this multi-species inversion is to provide better estimates of anthropogenic emissions, and, in the case of CO_2, to better separate the biospheric from anthropogenic contributions. This paper is structured as follows: a short description of the different components of the modeling framework is given in Sect. 2; in Sect. 3 we present and discuss our results; Sect. 4 gives the conclusions.

Christoph Gerbig 18.12.17 16:05
Gelöscht: .

Christoph Gerbig 19.12.17 09:12
Gelöscht: from

2. Material and Methods

2.1 Modeling framework

Before describing the different models composing the modeling framework, we introduce some specific terminology to reduce ambiguity in Sect. 2.1.1-2.1.6. Quantities that can be observed are termed *species*, or *trace gases*, corresponding in this case to total CO_2, CO and CH_4. These three species are simulated using five *modeled species*, namely CO_2 from fossil fuels, CO_2 related to GEE (Gross Ecosystem Exchange) and to respiration, CO, CH_4. Modeled species related to anthropogenic emissions are modeled as the sum of contributions from different *emission sectors* (Table 1) and *fuel types* (Table 2); as a further factor of discrimination, both anthropogenic and biospheric contributions are split into monthly contributions. Simulated fluxes specific for different modeled species, emission sectors, fuel types and months of the year are called *flux categories*. In this Material and Methods section, a brief description of the different models that make up the modeling framework is given. For more detailed information, see Boschetti (2015).

Christoph Gerbig 18.12.17 16:05
Gelöscht: Matherial

2.1.1 Vertical profile input data

In this study the modeled profiles have the identical structure to those collected from the IAGOS fleet of commercial airliners. More precisely, the spatial and temporal coordinates of different observations will be used as input for the modeling framework whereas the observed values of atmospheric mixing ratios of CO and meteorological parameters themselves will play a role in calibrating the modeling framework.

Central for this work is the concept of the Mixed Layer (ML), the lower part of the troposphere in which trace gases are well mixed due to turbulent convection in the time scale of an hour or less, and in which the effect of regional surface-atmosphere fluxes is the strongest. As input to the inversion we use the enhancement of the species' mixing ratio within the mixed layer relative to that in the free troposphere (FT), similar to the approach described in Boschetti (2015). This mixed layer enhancement best reflects the influence of regional fluxes. To compute this, we take the average mixing ratio within the mixed layer and subtract the value taken at 2 km above the mixed layer top (z_i), i.e. well within the free troposphere. The z_i is a very important parameter in atmospheric modeling, and accounts for most of the transport uncertainty in the vertical domain. In fact, assuming that the mixed layer is the part of the troposphere in which trace gases are well mixed due to turbulent convection, given a certain amount of trace gas in the ML, its mixing ratio depends strongly on its depth z_i. More precisely, even if the model has correctly reproduced the amount of trace gas in the real mixed layer, if the modeled z_i is lower (higher) than the actual one, then the simulated ML mixing ratio will be higher (lower) than it actually should be. In the present study, modeled z_i are corrected according to Boschetti (2015, Sect. 2.2.1)

2.1.2 Transport-flux coupling

The modeling framework is composed of a regional transport model (STILT), the EDGAR (Emission Database for Global Atmospheric Research) emission inventory to model anthropogenic emissions, VPRM (Vegetation Photosynthesis and Respiration Model) to model emissions from the biosphere and output from global transport models for lateral boundary conditions for the different modeled species. The expressions 'anthropogenic emissions' and 'fossil fuel emissions' are considered synonymous in this paper and are used to indicate the sum of fossil fuel and biofuel emissions, without including contributions from LULUCF (Land Use, Land use Change and Forestry).

For regional transport we make use of the LPDM STILT (Stochastic Time-Inverted Lagrangian Transport) (Lin, 2003) to derive the sensitivity of the atmospheric mixing ratio measurement to upstream surface-atmosphere fluxes, so-called "footprints". Briefly, for each measurement location and time (also called receptor point), the model releases an ensemble of virtual particles that are driven back in time using wind fields from ECMWF and turbulence as stochastic process; the residence time within the lower half of the mixed layer is used to determine the potential contribution from surface fluxes, and the cumulative sum of these contributions determines the footprint, that identifies the part of the domain with a certain influence on a single receptor point. To represent the mixed layer enhancements, the footprints for receptors within the boundary layer are averaged, and the footprint for the free tropospheric receptor is subtracted from this, resulting in a footprint for the mixed layer enhancements. This footprint is then matrix-multiplied with an emission map from an emission inventory, resulting in a simulated mixing ratio enhancement corresponding to the regional contribution at the measurement location.

A detailed description of STILT is given in Lin (2003) and Gerbig (2003). We use STILT coupled with emission models for both anthropogenic (EDGAR) and biosphere (VPRM) fluxes on a regional domain that covers most of Europe (33° to 72° N,

Christoph Gerbig 18.12.17 16:05

Gelöscht: For each measurement location and time (also called receptor point), a single footprint is derived; this

-15° to 35° E) with a spatial resolution of 1/8 degree for latitude and 1/12 degree for longitude, roughly corresponding to 10 km. As lateral boundary condition for CO mixing ratios the MACC reanalysis (Inness, 2013, downloaded from http://www.ecmwf.int) was used, whereas for CO_2 and CH_4 we use output from the Jena CarboScope (Rödenbeck, 2003; CO_2 data available from www.bgc-jena.mpg.de/CarboScope/) which is based on forward simulations of global-inversion optimized fluxes with the TM3 transport model (Heimann and Körner, 2003). TM3 fields have lower resolution, but they are chosen for their consistency with measurements from the ground-based network. In addition, spatial resolution is of relatively minor importance for the contribution from the lateral boundary as it is far away from the measurement locations.

For fossil fuel emissions we use a model based on the EDGAR emission inventory modified following the same approach taken for COFFEE (CO_2 release and Oxygen uptake from Fossil Fuel Emission Estimate) (Steinbach, 2011,; Vardag, 2015). More precisely, to obtain hourly resolved emissions from the original EDGAR annual fluxes for different emission categories we add specific temporal activity factors (Denier van der Gon, 2011) to account for differences in emissions due to seasonal, weekly and daily cycles. In addition, the different emission categories are further split into contributions from different fuel types from British Petroleum's Statistical Review of World Energy 2014 (BP, 2014). The World Energy Outlook from IEA as alternative source of information was not chosen, as the report from BP is available earlier (April vs. November of the following year). This allows for taking into account changes in emissions between different years. Such an emission model provides hourly resolved fluxes for each fossil fuel flux category with a spatial resolution of roughly 10 km on our regional European domain. For each of the three anthropogenic modeled species (CO_2, CO and CH_4), different emission maps are used as input. Temporal profiles are then applied to these sector- and fuel-specific emission maps. To take into account also the contribution from the biosphere we use the Vegetation Photosynthesis and Respiration Model (VPRM). VPRM simulates realistic patterns at small spatial (10 km x 10 km) and temporal (hourly) scales and is used here to provide the a priori fluxes for biosphere-atmosphere exchange of CO_2. This model is described in detail in Mahadevan (2008).

STILT transport is driven by meteorological fields from the ECMWF IFS (12 hour forecasts twice daily at 3-hourly temporal resolution), which have a spatial resolution of 0.25 degree with 61 vertical levels. In the following, we will refer to the STILT/EDGAR/VPRM/MACC/TM3 combination of transport, simulated fluxes and advected boundary conditions as merely 'STILT' for simplicity.

2.1.3 Bayesian inversion

Atmospheric inversions provide an estimate of the distribution of sources and sinks over the domain's surface from available concentration measurements ("top-down" approach). This can be formalized in the following linear relation:

$$\boldsymbol{y} = \mathbf{K}\boldsymbol{\lambda} + \boldsymbol{\varepsilon} \quad (1)$$

Where the $\boldsymbol{y}$ vector contains the n observations, and $\mathbf{K}$ is the Jacobian matrix that relates the observations with the state vector $\boldsymbol{\lambda}$. In the present study the focus will be on surface-atmosphere gas exchanges due to both biospheric processes and anthropogenic emissions. So the observations are trace gas mixing ratios at different times and locations, $\mathbf{K}$ is the product of a transport operator $\mathbf{H}$ that maps flux sensitivities at different times and locations with a set of gridded fluxes $\mathbf{F}$ for the categories of interest, while the state vector $\boldsymbol{\lambda}$ contains the m scaling factors for the flux categories of interest. $\mathbf{H}$ has n rows and a number of column equal to $h=N_x*N_y*N_t*N_s$ being respectively the number of pixels in the emission model along the x and y axes, the number of (hourly) simulations in the whole year of interest and the number of state vector elements, resulting in a huge matrix. As the matrix $\mathbf{F}$ describes the different simulated gridded fluxes, it is comparably large and has h rows and m columns. By considering K as the result of the product of these two large matrices, it is possible to limit its dimensions to only n rows and m columns; this allows for simplifying the critical task of relating observation with simulated fluxes of the categories of interest. The state vector accounts for specific emission sectors (Table 1) and fuel types (Table 2) for each one of the three modeled species from the EDGAR emission model, plus gross fluxes (gross ecosystem exchange GEE and respiration R) modeled by VPRM for 5 different vegetation classes. For both anthropogenic and biospheric fluxes the temporal resolution of the state vector is monthly. The number of state vector elements per month amounts to 69 scaling factors for the different fuel- and sector-specific anthropogenic emissions for each species, and 10 scaling factors for biosphere-atmosphere exchange (respiration and photosynthesis for each of the five vegetation classes), so in total 217 scaling factors per month, or 2604 scaling factors for the full year. To avoid large memory requirements for $\mathbf{H}$ and $\mathbf{F}$ matrices, their product is directly computed within the STILT code. The random error $\boldsymbol{\varepsilon}$ accounts for measurement error related to uncertainty in the observation and to model-data mismatch resulting from model uncertainty.

Bayesian inversion combines observations (IAGOS profiles) with a priori information (scaling factors and their a priori uncertainties) to reconstruct the most probable state vector. Optimum posterior estimates of the scaling factors are obtained by minimizing the following cost function J (Rodgers, 2000):

$$J(\boldsymbol{\lambda}) = (\boldsymbol{y} - \mathbf{K}\boldsymbol{\lambda})^T \mathbf{S}_{\boldsymbol{\varepsilon}}^{-1}(\boldsymbol{y} - \mathbf{K}\boldsymbol{\lambda}) + \left(\boldsymbol{\lambda} - \boldsymbol{\lambda}_{prior}\right)^T \mathbf{S}_{\mathbf{prior}}^{-1}(\boldsymbol{\lambda} - \boldsymbol{\lambda}_{prior}) \tag{2}$$

Here the first and the second term are the observational constraint and the prior constraint term respectively. The prior scaling factors for the fluxes of the different tracers are set equal to one. $\mathbf{S}_{\boldsymbol{\varepsilon}}$ is the error covariance matrix for the mismatch between simulated and observed mole fractions (model-data mismatch) and accounts for instrumental uncertainty, uncertainty related to the transport model, and other sources of uncertainty like boundary conditions and flux aggregation not accounted for through the state vector adjustment. $\mathbf{S}_{\mathbf{prior}}$ is the error covariance matrix for the prior scaling factor; its implementation requires a different approach for biospheric and anthropogenic fluxes. The detailed error structure for model-data mismatch and prior uncertainty is described in the Sect. 2.1.4. Minimizing the cost function results in an optimal posterior estimate of the state vector $\boldsymbol{\lambda}$ that is consistent with both the measurements and the prior model estimates:

$$\hat{\boldsymbol{\lambda}} = \left(\mathbf{K}^{\mathbf{T}}\mathbf{S}_{\varepsilon}^{-1}\mathbf{K} + \mathbf{S}_{\mathbf{prior}}^{-1}\right)^{-1}\left(\mathbf{K}^{\mathbf{T}}\mathbf{S}_{\varepsilon}^{-1}\boldsymbol{y} + \mathbf{S}_{\mathbf{prior}}^{-1}\boldsymbol{\lambda}\right) \quad (3)$$

The error covariance matrix of the optimal posterior state (the posterior uncertainty) is given by:

$$\mathbf{S}_{\mathbf{post}} = \left(\mathbf{K}^{\mathbf{T}}\mathbf{S}_{\varepsilon}^{-1}\mathbf{K} + \mathbf{S}_{\mathbf{prior}}^{-1}\right)^{-1} \quad (4)$$

Note that this quantity depends on neither the prior fluxes nor the measured mixing ratios, but only on their respective uncertainties and on the transport matrix **K**. In this study, the inverse of the matrices was calculated using the R-function ‘solve‘ from the base package of R version 3.0.0 (http://www.r-project.org/).

The targeted quantities of this study are the aggregated emissions over a specific area at a specific time scale (e.g. month); those quantities can be derived from the prior and posterior state through a spatiotemporal aggregation operator **A** that allows for the conversion of scaling factors into physically representative quantities. As the pseudo-observations are clustered around a single location (Frankfurt), fluxes over the whole European domain can very likely not be constrained. Therefore, as a spatial aggregation scale we chose an area from which fluxes have a significant contribution to the observations made at Frankfurt. For this we compute the temporally accumulated footprint values (cf. Sect. 2.1.2) for the whole year 2011, and select those spatial pixels that correspond to 50% of the total (spatially integrated) footprint (Fig. 1). Note that by using this aggregation scale we assume perfectly-known distribution within a given flux category that can result in aggregation error, especially with respect to biogenic fluxes, that are not so well known as anthropogenic fluxes. However, the chosen domain of aggregation is quite small, and the total anthropogenic fluxes are divided according to species, emission categories, fuel types and months. This result in 69 degrees of freedom per month for each anthropogenic species and 10 degrees of freedom per month for the biospheric fluxes; for this reason we expect the aggregation error not to be a particularly important source of uncertainty. The prior and posterior uncertainty of these targeted quantities (σ_{prior} and σ_{post}) is obtained by applying the aggregation operator to the respective uncertainty covariances:

$$\boldsymbol{\sigma}_{\boldsymbol{prior}} = \sqrt{\mathbf{A}^{\mathbf{T}}\mathbf{S}_{\boldsymbol{prior}}\mathbf{A}} \quad \text{and} \quad \boldsymbol{\sigma}_{\boldsymbol{post}} = \sqrt{\mathbf{A}^{\mathbf{T}}\mathbf{S}_{\boldsymbol{post}}\mathbf{A}} \quad (5)$$

Different versions of the aggregation operator were created for this: emissions categories are aggregated according to different fuel types (coal, oil, gas, bio, waste, other) and according to emission sectors (energy, transport, industry, buildings,

Christoph Gerbig 18.12.17 16:05
Gelöscht: $= (\mathbf{K}^{\mathbf{T}}\mathbf{S}_{\varepsilon}^{-1}\mathbf{K} + \mathbf{S}_{\mathbf{prior}}^{-1})(\mathbf{K}^{\mathbf{T}}$

Christoph Gerbig 18.12.17 16:05
Gelöscht: .

Christoph Gerbig 19.12.17 09:02
Gelöscht: As

Christoph Gerbig 18.12.17 16:40
Gelöscht: a domain encircling the 50% influence in the cumulated footprint for the receptor points in the ML for the year 2011

agriculture, waste, fossil fuel fires). Note that only these aggregated fluxes are optimized, not the individual gridded fluxes of the emission inventories.

To quantitatively assess the information provided by the inversion, the reduction of uncertainty in the posterior compared to the prior estimate is a useful measure. The uncertainty reduction *UR* is defined as:

$$UR = 1 - \frac{\sigma_{post}}{\sigma_{prior}} \quad (6)$$

The uncertainty reduction ranges from 0 (posterior as large as the prior uncertainty) to 1 (posterior negligible compared to the prior uncertainty).

2.1.4 Prior error structure

As in this study a multi-species inversion with CO, CO_2 and CH_4 is envisioned, we have the chance to exploit the correlations in the uncertainties of the different trace gases related to both a priori fluxes and model-data mismatch. This is particularly true for CO and CO_2 because they share a larger part of the emission sources, which implies correlations in the respective uncertainties. In the multi-species inversion, such information is stored in the areas of the error covariance matrices that describe covariance between different modeled species (off-diagonal 'blocks' in Fig. 2b for $\mathbf{S_{prior}}$ and Fig. 3b for $\mathbf{S_\varepsilon}$). In the single-species inversions, said covariance is set to zero, corresponding to a situation where the different species are completely independent of one another. Conversely, the measurement uncertainty is stored in the main diagonal of the $\mathbf{S_\varepsilon}$ (Fig. 3d).

We used a single year (2011) dataset restricted to the vertical profiles centered at the Frankfurt airport, and restricted to daytime during well-mixed atmospheric conditions (10:30 to 17:30 CET). The dataset contains 1098 pseudo-observations, 366 for each of the three observable species, whereas the state vector contains the scaling factors for 2604 flux categories, each equal to one in the prior.

The prior error covariance matrix can be expressed as follows:

$$\mathbf{S_{prior}} = \mathbf{C_{prior}}\boldsymbol{\rho}_{\mathbf{prior}} \quad (7)$$

where $\mathbf{C_{prior}}$ is the prior error correlation matrix (Fig. 2a) and $\boldsymbol{\rho}_{\mathbf{prior}}$ is a prior rescaling matrix described in Sect. 2.1.5 (Fig. 4a). First we describe how $\mathbf{C_{prior}}$ is generated. The prior error correlation matrix is a square matrix of rank 2604, reflecting

Christoph Gerbig 18.12.17 16:05
Gelöscht: 6

the length of the state vector, and results from the product of three components (Fig. 2b, 2c and 2d) accounting for correlations between flux categories according to the modeled species, emission sectors and fuel types respectively. In four different instances, a correlation of 0.7 is applied:

1. Between different anthropogenic modeled species
2. Between GEE and respiration
3. Between different emission sectors
4. Between different fuel types

Such a correlation implies that the explained variance for each constraint everything else being equal is roughly 50%, (0.7 to the square equals 0.49) with the rest remaining independent. In addition, the correlation between fossil-fuel-related and biosphere-related scaling factors is zero, and the same holds for fluxes of different months, indicating complete independence from one another. In this study, we assume a certain annual total domain wide flux uncertainty, and then break it down by sectors, fuels, and months by inflating the error. By assuming no correlation between different months we ensure maximum flexibility in the system to retrieve month-to-month changes based on the observations. Assuming correlation between months would be possible, but has not been investigated here. It is unclear how good the seasonal variation in emissions from the inventories actually is, so in order to not rely too much on these we chose zero correlation. Investigating the effects of different correlation set-ups for the seasonal cycle could be the focus of future research.

2.1.5 Prior error scaling

After having specified the prior error correlation matrix $\mathbf{C_{prior}}$, we now describe how we rescale it to obtain $\mathbf{S_{prior}}$; for this task we rewrite Eq. (7) as

$$\mathbf{S_{prior}} = \mathbf{C_{prior}} \boldsymbol{\rho}_{\mathbf{prior}} = \tag{8}$$

$$= \begin{pmatrix} \boldsymbol{C_{11}} & \boldsymbol{C_{12}} & \boldsymbol{C_{13}} & \mathbf{0} \\ \boldsymbol{C_{21}} & \boldsymbol{C_{22}} & \boldsymbol{C_{23}} & \mathbf{0} \\ \boldsymbol{C_{31}} & \boldsymbol{C_{32}} & \boldsymbol{C_{33}} & \mathbf{0} \\ \mathbf{0} & \mathbf{0} & \mathbf{0} & \boldsymbol{C_{bio}} \end{pmatrix} \begin{pmatrix} 1/\rho_1\rho_1 & 1/\rho_1\rho_2 & 1/\rho_1\rho_3 & 0 \\ 1/\rho_2\rho_1 & 1/\rho_2\rho_2 & 1/\rho_2\rho_3 & 0 \\ 1/\rho_3\rho_1 & 1/\rho_3\rho_2 & 1/\rho_3\rho_3 & 0 \\ 0 & 0 & 0 & \rho_{bio}^2 \end{pmatrix}$$

where each $\mathbf{C_{ij}}$ is a subset of the fossil fuel part of $\mathbf{C_{prior}}$ ('block') as shown in Fig. 2, and each ρ_i is defined as

$$\rho_i = \sqrt{\frac{A_i'^T \mathrm{C_{ii}} A_i'}{\left(\sum_j A_{ij}' \, \varepsilon_i\right)^2}} \tag{9}$$

where **A'** is the aggregation operator for annual fluxes over the full domain, and ε_i is the corresponding relative prior uncertainty, assuming the values specified in Table 3 for different cases. Case 1 is considered as the default case, with prior uncertainty values conservatively assumed to be 20%, for CO_2 and 50% for CO and CH_4. Conversely, $\mathbf{C_{bio}}$ covers the biosphere part of $\mathbf{C_{prior}}$, and for $\sum A_i' \varepsilon_i$ for ρ_{bio} we use a prior uncertainty of 0.54 GtC y^{-1}, as derived in Panagiotis (2016) for the VPRM model. The biospheric part of the prior error covariance matrix assumes no correlation with the fossil fuel species.

The posterior of each Bayesian inversion depends on its specific prior. As the multi- and single-species inversion have different prior uncertainty structures, the uncertainty reduction for targeted quantities cannot be directly compared (Eq. (4)). To be able to compare the two inversions, we require that the a priori aggregated uncertainty of the targeted quantities remains the same, and distribute it differently each time; the prior rescaling matrix $\boldsymbol{\rho}_{\mathbf{prior}}$ is needed for this task. The benefits were tested for observations taken in different months and for three different error structures in the prior uncertainty. As a priori aggregated uncertainty we use a percentage of the aggregated modeled emissions for fossil fuels across the whole year. Table 3 shows the percentage values used for different cases.

2.1.6 Model-data mismatch error structure

In an atmospheric inversion, the model-data mismatch from every uncertainty source (such as measurement uncertainty, transport model uncertainty, spatial representation error due to limited model resolution, and boundary condition inaccuracies) needs to be taken into account. In our inversion scheme, we parameterize both the transport model uncertainty and the measurement uncertainty, with the latter playing a minor role. The model-data mismatch covariance matrix ($\mathbf{S_\varepsilon}$) is constructed according to the following equation:

$$\mathbf{S_\varepsilon} = \mathbf{C}_s \mathbf{C_t} \boldsymbol{\varepsilon}_{tran}^2 + \boldsymbol{\varepsilon}_{meas}^2 \tag{10}$$

where $\mathbf{C_s}$ accounts for correlations between different observed species (Fig. 3b), $\mathbf{C_t}$ accounts for the temporal correlation (Fig. 3c), $\boldsymbol{\varepsilon}_{tran}$ is the total transport error and $\boldsymbol{\varepsilon}^2_{\mathbf{meas}}$ accounts for all of the non-transport related errors like spatial representation error and lateral boundary conditions (Fig. 3d).

The assumed measurement uncertainty is 1 ppm for CO_2, 20 ppb for CO and 20 ppb for CH_4, while ε_{tran} is time dependent and assumed to be proportional to the modeled enhancement due to regional fluxes. The assumed measurement uncertainty is higher than the expected instrument precision because it also includes in addition the uncertainties related to spatial representation and lateral boundary condition. ε_{tran} is characterized as follows by different components in the vertical and horizontal domain:

$$\varepsilon_{tran} = enh\sqrt{\left(\varepsilon_{tran\_h}^2 + \varepsilon_{tran\_v}^2\right)} \tag{11}$$

where *enh* indicates the modelled enhancement, and both the horizontal transport error ε_{tran_h} and the vertical transport error ε_{tran_v} are characterized as percentage error; ε_{tran_h} is assumed to be 50%, while ε_{tran_v} is a profile-specific relative error with a mean value of about 10%. The vertical transport error accounts for the fact that the shallower the mixed layer is, the more difficult it is to model the atmosphere. We assume that after zi-correction the remaining error is on the order of 50 m (related to the vertical resolution of the profile data), so the relative error ε_{tran_v} is assumed as the ratio of 50 m to the modeled z_i; in this way we obtain an error that gets larger the shallower the mixed layer is. For the horizontal component, an uncertainty of 50% is a conservative estimate based on Lin and Gerbig (2005), where the horizontal transport error is found to be 5.9 ppm for CO_2. This, combined with about 10 ppm of drawdown in the mixed layer relative to the free troposphere, gives something like 50% error in the regional flux signal. The vertical component is so much smaller in percentage since the simulated mixing ratios are already corrected for mismatch between modeled and observed z_i.

In the multi-species inversion, the transport error correlation across species is 0.7 (Fig. 3b), while in the single-species inversion this is set to zero. Time correlation is assumed to decay exponentially with an exponential constant of 12 hours. The between-species correlation for model-data mismatch related to transport uncertainty reflects the fact that species are partially co-emitted and share the same atmospheric transport (and its related uncertainty).

2.2 Synthetic experiment

2.2.1 Pseudo-data generation

As explained in the introduction, in situ measurements are not available for all of the three trace gases of interest, but only for CO. For this reason this paper aims to evaluate the benefits of a multi-species inversion over a corresponding single-species one by performing a synthetic experiment, using pseudo-observations derived by perturbation of the model outputs based on a priori state vector values. More precisely, the pseudo-observation vector is obtained by matrix multiplication between the Jacobian matrix **K** and what we assume to be the true state vector. The true state vector itself is obtained by using the sum of the prior state vector (all values equal to one) and a random realization of the prior error, truncated to avoid

Christoph Gerbig 18.12.17 16:05
Gelöscht: where

Christoph Gerbig 18.12.17 16:59
Gelöscht: . More precisely,

Christoph Gerbig 18.12.17 17:01
Gelöscht: related to the modeled z_i

Christoph Gerbig 18.12.17 17:03
Gelöscht: difference in vertical resolution between the transport model and the IAGOS profiles, and its mean value is about 10%.

negative state vector values. In detail, the error realization is obtained by multiplying a randomly generated, normally distributed vector with the prior error covariance matrix. This ensures that such realization has the same error correlation of the prior uncertainty. Where the result of such matrix-vector product is negative, the same operation is performed recursively until all elements of the state vector are positive. This ensures that the difference between the true and prior state vector has the same error correlation structure as described by the prior error covariance matrix.

3. Results and Discussion

Before evaluating the performance of the inversion scheme in reducing the uncertainty of the state space, a closer look at the ability of the modeling framework to reproduce the enhancements is necessary. Unfortunately, this can be done only for CO as actual measurements are not available for the other species. Figure 5 shows the mean daily enhancement of the three fossil fuel species for both observations and model outputs using prior emissions. A common feature to the three trace gases is that lower values tend to occur during summer time due to a better mixing of the atmosphere. Conversely, enhancement values tend to be higher during winter, reflecting the more stratified atmosphere of the cold months.

Christoph Gerbig 18.12.17 17:16
Gelöscht: model outputs and

In Fig. 5 the modeled CO plot was multiplied by a factor of 2.8, corresponding to the mean ratio between observed and modeled CO enhancements, similar to what was found in Boschetti (2015). Mixing ratio values are highly variable, but the model produces a good indication of the temporal variation of the ML enhancement; the squared correlation coefficient between observed and modeled CO enhancements is 0.62, while the standard deviation of corrected model and observation residuals is 85 ppb; note that by not accounting for the z_i correction, such values would be 0.56 and 87 ppb respectively. The median of the mixing ratio enhancement for the three trace gases is 2.8 ppm for CO_2, 18.6 ppb for CO and 26.6 ppb for CH_4. For CO_2 this seasonal difference is enhanced due to the simultaneous presence of both anthropogenic and biogenic emissions. During summer values are slightly negative due to strong photosynthesis fluxes from growing vegetation from the active combined with deeper vertical mixing. Negative values arise in 31% of the cases predominantly during the warmer months, implying that during the growing period uptake by photosynthesis dominates over release from combustion and respiration. Both CO and CH_4 experience higher values during winter due to the shallow mixed layer usually associated with cold temperatures, and lower values during summer as higher temperature cause the mixed layer to reach higher altitudes; differences related to seasonal domestic heating and transportation may also play a role. In addition, enhancement for both species is occasionally negative, most likely owing to advection of polluted air masses in the free troposphere. An alternative explanation is that strong winds at lower heights can disperse the emissions in the boundary layer and create a situation in which the mixing ratio in the FT is higher than in the ML.

Christoph Gerbig 18.12.17 16:25
Gelöscht: usually manages to reproduce the associated spikes; the squared correlation coefficient between observed and modeled CO enhancements is 0.56 and the standard deviation of corrected model and observation residuals is 87 ppb. The median of the mixing ratio enhancement for the three trace gases is 30.0 ppb for CO, 53.7 ppb for CH_4 and 3.0 ppm for CO_2

Figure 6 shows the prior and posterior error covariance matrices for the base multi-species inversion. Note that CO_2 from anthropogenic emissions is assumed to be independent from biogenic emissions; therefore prior error correlation between these categories is zero. The posterior error covariance matrix for the multi-species inversion (Fig. 6b) shows lower values corresponding to an average uncertainty reduction of 23% across all state vector elements, while the posterior error covariance matrix for the single-species inversion (not shown) is characterized by a mean uncertainty reduction of 20%. This result implies that the multi-species inversion improves the uncertainty reduction by roughly 15%. Negative values in the posterior error correlation matrix are to be expected because different categories are bind together by correlations and therefore are not free to vary independently.

Figure 7 and 8 show a priori, a posteriori, and "true" fluxes related to different aggregated fuel types and to different emission categories as described in Tables 1 and 2 for the months of July and December. Figure 8 also shows the biospheric contribution (as absolute values) scaled down by a factor of 10. As is to be expected, the biospheric contributions show strong differences according to the seasonal cycle, while anthropogenic emissions remain rather stable. However, it is worth pointing out that while the fossil fuel prior is similar for both months, the assumed truth can be rather different due the random assignment of the prior error realization. In most cases, the posterior adapts and is therefore closer to the truth than the prior; the posterior uncertainty is also visibly reduced, as expected. Regarding the different tracers, CO_2 and CO show a somewhat similar pattern indicating a partial overlap in dominating emission categories while CH_4 is dominated by different contributions in both fuel types and emission categories.

Our modeling framework is currently not well suited to account for unreported sources of CH_4 due to the lack of information about natural gas and oil production operations, or from recent and old mining areas.. Many recent studies have discussed the problem, mainly referring to shale basins exploited via hydraulic fracturing in the US (e.g. Kort et al., 2016; Karion et. al, 2015; Lyon et al., 2015). For example, Karion (2015) concludes that EDGAR underestimates methane emissions associated with oil and gas industry by a factor of 5 in the US. However, the situation over the European continent may be quite different. In a review about risk assessment of shale gas development in the UK, Prpich (2015) reports that the European Union is generally much more cautious about unconventional oil and gas sources, while a recent study on a methane plume over the North Sea (Cain et al., 2017) concluded that the bulk signature of said plume originated from on-shore coal mines and power stations in the Yorkshire area.

In general, the absence of some emission sources in an inventory is equivalent to the assumption of having point sources not included in the emission map, but still contributing to the measurements. The inversion scheme would typically react to this by assigning such point sources in some other sector other fuel type. As a result, the posterior enhancements would be biased low in proximity of that point sources, and (slightly) biased high for influences from other regions with the same sector or

Christoph Gerbig 18.12.17 16:05
Gelöscht: With respect to the prior error covariance matrix, the posterior error covariance shows lower values (Fig. 6) corresponding to an uncertainty reduction of 22%.

Christoph Gerbig 19.12.17 09:35
Formatiert: Schriftart:Kursiv

fuel type. This issue should definitely be considered in a future study making use of actual CO, CO_2 and CH_4 observations from IAGOS but has limited effects on this paper, as our main focus is on the benefits of inter-species correlation on the posterior uncertainty in the frame of a synthetic experiment

Note that our modeling framework does not allow for simulating CO biogenic fluxes during the growing season. Warm days in summer correspond to large amount of biogenic VOC's being emitted from the vegetation, producing CO to non-negligible levels. According to Hudman (2008), anthropogenic emissions accounts for only 31% of CO emissions in the US during summer. Conversely, according to estimates from EDGAR, CO anthropogenic emissions during summer are about 18% of the annual anthropogenic emissions. Combining these two results, one could conclude that CO production from biogenic sources accounts for roughly 42% of total annual CO emissions.
In general, the absence of some emission sources in an inventory is equivalent to the assumption of having point sources not included in the emission map, but still contributing to the measurements. The inversion scheme would typically react to this by assigning such point sources in some other sector other fuel type. As a result, the posterior enhancements would be biased low in proximity of that point sources, and (slightly) biased high for influences from other regions with the same sector or fuel type. This issue should definitely be considered in a future study making use of actual CO, CO_2 and CH_4 observations from IAGOS but has limited effects on this paper, as our main focus is on the benefits of inter-species correlation on the posterior uncertainty in the frame of a synthetic experiment.

CO_2 and CO are dominated by combustion sectors (Fig. 8). The most important emission sectors for CO_2 are energy, industry, transport and building, each contributing 7-10 MtC month^{-1} in July and 6-14 MtC month^{-1} in December. Dominant fuels (Fig. 7) for CO_2 are coal, gas and oil, whose prior fluxes (pseudo data) have a magnitude of 6-11 Megatons of carbon per year (MtC month^{-1}) in July and 8-14 MtC month^{-1} in December. For CO the most important emission sector is heating of buildings during winter contributing a 0.19 MtC month^{-1} flux with only secondary contributions from industry and transport with a magnitude of 0.04 MtC month^{-1} and 0.05 MtC month^{-1} respectively (during July and December). The dominant fuel for CO is biofuel with 0.19 MtC month^{-1} emissions during winter. The secondary industrial and transport contributions originate in summer from oil and biofuels with a magnitude of 0.06-0.08 MtC month^{-1} and from agricultural waste burning with a magnitude of 0.06-0.11 MtC month^{-1}.

Contrary to CO_2 and CO, CH_4 is determined by non-combustion sectors, more specifically by a contribution of 0.15 MtC month^{-1} flux from agriculture (manure management and rice cultivation) in July with secondary contributions from waste and energy with a magnitude of roughly 0.06-0.08 MtC month^{-1} in both July and December. Other non-combustion sectors, in particular wastewater treatment and landfills contribute to a total of 0.16-0.24 MtC month^{-1} of emissions. These non-combustion sectors contribute to less than 20% of total CO_2 emissions, with 1.13 MtC month^{-1} from the cement and lime industry and less than 20% to the total CO emissions (0.03 MtC month^{-1} from the metal industry).

The contribution to CO_2 from biospheric primary production (a sink for atmospheric CO_2) is about 100 MtC month^{-1} in July, which drops to almost zero in December, while respiration values are 50 MtC month^{-1} in July and roughly 15 MtC month^{-1} in December.

As further assessment of the inversion performance, we tested the ability of the inversion scheme to capture the truth compared with a perturbed version of the prior. Such perturbed version is obtained by adding a random distribution with mean and standard deviation equal one to the prior state space, similar to how the truth is obtained. For each simulated species we calculated the total annual fluxes for prior, posterior, truth, and perturbed prior. From these total fluxes we then derive the overall residual between prior and truth, posterior and truth, and perturbed prior and truth. It is clear from Table 4 that while the overall bias between posterior and truth is lower than the prior-truth bias, the bias between perturbed prior and truth is much higher, implying that the performance of the inversion is not an artifact of the pseudo-data generation. In addition, it was found that the truth-posterior bias of the multi-species inversion is mostly slightly lower compared to the single-species inversion. Such difference is between -2.2% and 7.6%, according to the simulated species, with an overall value of 0.3%.

Improper characterization of the error correlation may result in systematic bias in the posterior estimate. As mentioned in Sect. 2.1.6, inter-species correlation, the correlation between different fuel types and the correlation between different emission sectors in $\mathbf{S}_{\mathbf{prior}}$ is assumed equal to 0.7 (Sect. 2.1.4). To assess how well the system will reproduce the 'true' fluxes with incorrectly specified correlations, a series of experiments was performed in which the inter-species correlation in $\mathbf{S}_{\varepsilon}$ remains equal to 0.7, while the three correlation coefficients in $\mathbf{S}_{\mathbf{prior}}$ assume different values ranging from 0.1 to 0.9. Table 5 shows the residuals between total annual posterior fluxes and total annual true fluxes for the five simulated species, derived similarly as for Table 4. We found that for all species the uncertainty reduction increases with correlation. More precisely, from correlation 0.1 to 0.9, the annual uncertainty reduction for anthropogenic CO_2 increases from 26.6% to 51.7%, while the increase is lower for GEE (from 72.4% to 73.1%) and respiration (from 39.3% to 41.3%) because the biospheric fluxes are independent from other species. For CO, the uncertainty reduction increases from 60.7% (with correlation 0.1) to 66.4% (with correlation 0.9). The annual uncertainty reduction for CH_4 increases from 60.5% to 67.5%.

In addition, the posterior-truth biases are always lower than the prior-truth biases. The posterior uncertainty values (1-sigma) are usually larger then the corresponding bias values as expected, except for CO and for CH_4 with prior correlations equal to 0.9. Thus the posterior is not significantly different from the truth. Conversely, the prior (not shown) is significantly different from the prior in the majority of cases for fossil fuel fluxes, and in some cases also for biogenic fluxes. The effect of assuming the incorrect error correlations appears to be in general small, possibly implying a relative robustness of our methods. Following this result, the fact that CH_4 is only partially co-emitted with CO_2 and CO should not affect the inversion in a strong way. For all of the experiments, the residuals between true and posterior fluxes are lower than residuals between

Christoph Gerbig 19.12.17 10:15
Gelöscht: Dominant fuels for CO_2 are coal, gas and oil, whose prior fluxes (pseudo data) have a magnitude of 6-11 Megatons of carbon per year (MtC y^{-1}) in July and 8-14 MtC y^{-1} in December, while CO is dominated by a 0.19 MtC y^{-1} flux from biofuels during winter and secondary contributions during summer from oil and biofuels with a magnitude of 0.06-0.08 MtC y^{-1}. Regarding CH_4, the single dominant contribution is from "Other" fuels, responsible for 0.16-0.24 MtC y^{-1} of emissions. "Other" fuel types include emissions from non-metallic minerals industry (e.g. cement, lime), agricultural waste burning, metal industry processing, chemical and solvent industry, solid waste disposal in landfills, wastewater treatment, manure management in agriculture, rice cultivation in agriculture, and agricultural soil emissions. For CO_2, the dominant contribution from these "Other" fuels in the European domain is from the non ... [1]

Christoph Gerbig 18.12.17 16:05
Gelöscht: To do so we calculated for each simulated species the overall bias for the wh ... [2]

Christoph Gerbig 19.12.17 12:47
Formatiert: Schriftart:Nicht Kursiv

Christoph Gerbig 19.12.17 12:47
Formatiert: Schriftart:Nicht Kursiv

Christoph Gerbig 19.12.17 12:47
Formatiert: Schriftart:Nicht Kursiv

Christoph Gerbig 19.12.17 12:47
Formatiert: Schriftart:Nicht Kursiv

Christoph Gerbig 19.12.17 12:47
Formatiert: Schriftart:Nicht Kursiv

Christoph Gerbig 19.12.17 12:47
Formatiert: Schriftart:Nicht Kursiv

Christoph Gerbig 19.12.17 12:47
Formatiert: Schriftart:Nicht Kursiv

Christoph Gerbig 19.12.17 12:47
Formatiert: Schriftart:Nicht Kursiv

Christoph Gerbig 19.12.17 12:47
Formatiert: Schriftart:Nicht Kursiv

Christoph Gerbig 19.12.17 12:47
Formatiert: Schriftart:Nicht Kursiv

Christoph Gerbig 19.12.17 12:47
Formatiert: Schriftart:Nicht Kursiv

Christoph Gerbig 19.12.17 12:47
Formatiert: Schriftart:Nicht Kursiv

Christoph Gerbig 19.12.17 12:47
Formatiert: Schriftart:Nicht Kursiv

Christoph Gerbig 19.12.17 12:51
Formatiert: Schriftart:Nicht Kursiv

true and prior fluxes for each of the simulated species; the difference between the cases with maximum and minimum residuals is around 4.2%. In addition, we found that the posterior aggregated fluxes in the nine experiments are not significantly different from each other, implying that the system is fairly robust against errors in the assumed inter-species correlation.

Before investigating the benefits of correlations between different tracers, it is meaningful to evaluate the uncertainty reduction in the monthly budgets for all five modeled species (Fig. 9, based on targeted spatial domain in Fig. 1). The first thing to note is that for all of the five trace gases the posterior uncertainty is lower than the prior one, as it should be. In addition, prior uncertainty varies through the year, reflecting modulation in emission fluxes obtained by adding activity factors to describe the seasonal, weekly and daily cycle.

Prior uncertainty assumes values around 0.4-0.6 MtC month^{-1} for CO_2, 5-15 ktC month^{-1} for CO, and 15 ktC month^{-1} for CH_4. For GEE the prior uncertainty is between 0.3 MtC month^{-1} and 46.7 MtC month^{-1}, and for respiration it is 5.1-19.0 MtC month^{-1}. Posterior uncertainty for CO_2 is 0.24-0.38 MtC month^{-1} for fossil fuel emissions, 0.3-9.9 MtC month^{-1} for GEE and 3.1-10.4 MtC month^{-1} for respiration, while it has a range of 3.3-4.7 ktC month^{-1} for CO and 2.7-7.0 ktC month^{-1} for CH_4. Mean uncertainty reduction of the monthly values is 38% for fossil fuels emission of CO_2, 41% for GEE, and roughly 45% for respiration, 63% for CO and about 67% for CH_4. It is worth pointing out that such values are higher than the mean uncertainty reduction in the scaling factors (23%); this happens because the most representative emission sectors are those influencing the observations the most and thus are also the most constrained.

In addition, note that in this case, the posterior uncertainties for single- and multi-species inversions are similar for the modeled species, with the exception of the CO_2 anthropogenic contributions. To generalize this last result, we tested the benefit of a multi-species inversion for the different cases of prior uncertainty values shown in Table 3. As an indicator for the benefit of including correlation between different species, we use the ratio between posterior uncertainty of the multi-species inversion and the posterior uncertainty of the corresponding single-species inversion. A value of one means that there is not benefit in adding an inter-species correlation to the inversion, while values greater than one means that a multi-species inversion is even less constrained than a single-species one. We expect this indicator to be less than one, meaning that inter-species correlations actually improve the constraint power of the inversion. As before, we consider here the uncertainties of the retrieved budgets for the 50% footprint, where the surface influence is strongest (Fig. 1). Values of this uncertainty ratio for the different trace gases as function of month are shown in Fig. 10 for the different cases listed in Table 3. The benefit of including inter-species correlations shown in Fig. 10 does not depend on different manifestations of the true fluxes, but only on the posterior uncertainty of the multi- and single-species inversions.

All of the species experience a reduction in the posterior uncertainty ratio due to the addition of inter-species correlation; said reduction is up to 20% for fossil fuel CO_2 and up to 10% for the other species; In addition, anthropogenic CO_2 is more

Christoph Gerbig 8.1.18 13:17
Gelöscht: y

Christoph Gerbig 18.12.17 16:05
Gelöscht: 64

Christoph Gerbig 18.12.17 16:05
Gelöscht: 22

sensitive to the prior relative error values than CO and CH_4. As the uncertainty of GEE and respiration is not modified, they show little to no variations for different cases (Fig. 10). There is a dependence of the benefit of the multi- over a single-species inversion on the prior uncertainty values (differences between cases 1-3), with the largest difference for fossil fuel emissions of CO_2. Interestingly for case 2 with reduced prior uncertainty for fossil fuel CO_2 emissions the benefit nearly doubles over the default case (Case 1). Also reducing the prior uncertainties of CO and CH_4 emissions (Case 3) more or less compensates for this increase in benefit. The reason for both of these results is probably to be searched in Eq. 8. In fact, changing the prior uncertainty in CO_2 emissions means to also change the off-diagonal blocks linking the different species together. However, by reducing the anthropogenic CO_2 uncertainty from 20% to 10% (Case 2), the diagonal block for CO_2 in the prior uncertainty changes by a factor four, while the off-diagonal blocks change only by a factor of two. This effectively ties the emissions of CO_2 tighter to the emissions of the other species, resulting in more benefit from a multi- over a single-species inversion. Conversely, when all prior uncertainties are reduced by a factor 2 (Case 3), both diagonal and off-diagonal blocks are reduced by a factor four. This explains why Case 1 and Case 3 show similar benefit values. Note that the assumed prior uncertainties for the default case (Case 1) are quite conservative, therefore lower uncertainties were chosen for Cases 2 and 3. While the absolute benefit of adding inter-species correlation is not a game-changer, it is worth pointing out that such improvement also comes with only slightly greater computational effort than multiple independent single-species inversions.

In order to assess the contribution of inter-species correlation in the prior uncertainty vs. that of model-data mismatch uncertainty, Fig. 11 also shows the resulting posterior uncertainty ratios for Case 1 (Table 3) from inversions only using prior or model-data mismatch correlation. For the anthropogenic component of CO_2, the greatest constraint is given by the prior correlation, while for GEE, respiration, and CH_4 the strongest contribution is from the model-data mismatch correlation. In the case of CO, the inter-species correlations for different components are dominant for different months of the year. What makes CO sensitive to different correlation structures during different seasons is that CO enhancement shows a stronger seasonal cycle compared to e.g. fossil fuel component of the CO_2 enhancement, with average values for January of around 150 ppb (25 ppm for CO_2), and for July of 9 ppb (4 ppm for CO_2). This results in a much weaker constraint on the CO emissions from the CO observations during summer, but still some constraint through the other species such as CO_2 via the a priori correlation in the emissions.

Palmer (2006) (in the following referred to as P06) studied the importance of inter-species correlation to improve inverse analysis using airborne data from the TRACE-P mission conducted in March/April 2001 over the western region of the Pacific Ocean. P06 derived a prior error correlation lower than 0.2 by analysing the uncertainty of emission factors from an Asia-specific emission inventory (Streets, 2003), which is significantly smaller than the correlation of 0.7 assumed in the present study. P06 deemed CO_2-CO prior correlation greater than 0.5 to be unrealistic for the emissions in Asia, which is mostly associated with the uncertainty in emission factors for CO of 67% for fossil fuel emissions and 240% for biofuel emissions in China (P06 Table 1). However, for the European region used in the present paper we argue that values around

0.7 are appropriate. The resulting uncertainty in the CO_2-CO ratio, diagnosed from the prior error covariance matrix used in this study, is about 50% for both biofuel and fossil fuel emissions in Europe, which we regard as reasonable. To compare results from P06 with those from the present study, ratios of posterior uncertainties resulting from inversions using correlations between CO_2 and CO of 0.7 in the prior uncertainties and to those using no correlations have been extracted from Fig. 7 in P06 and are also shown as orange diamonds in Fig. 11. It is easy to see that for anthropogenic CO_2, the value derived from P06 is higher than in our study, while the two values are very similar for CO. Similarly, posterior uncertainty ratios using model-data mismatch correlations of 0.7 between CO_2 and CO are derived from Fig. 8 of P06 and are shown as red diamonds. In this case, the value derived from P06 is slightly lower than in our study for anthropogenic CO_2, while the two are again very similar for CO.

Christoph Gerbig 18.12.17 16:05
Gelöscht: meaning,

From this comparison we can see that the estimates of the benefit of including inter-species correlation in atmospheric inversions in P06 and in this paper are on the same order of magnitude for anthropogenic CO_2 and almost identical for CO, suggesting a general continuity of results.

4. Conclusions

The present paper presents a synthetic experiment aiming to evaluate the effects of exploiting correlations between different trace gases in an atmospheric inversion. We quantitatively described the capability of the modeling framework to reproduce observations, the performance of the inversion scheme in reducing the uncertainty of the different trace gases, and the benefits of multi-species inversions compared to corresponding single-species inversions. We also describe a method to re-scale different prior uncertainty covariance matrices so that the corresponding posterior uncertainties are actually comparable.

Where possible, we confronted model outputs with available observations. Such comparison, possible only for CO, showed a good degree of agreement between the model and observations with an overall correlation of roughly 0.75; modeled values for CO enhancement underestimate the observed ones by a factor of roughly 2.8, compatible with what was found in

Boschetti (2015). It is found that posterior uncertainty is much lower than the prior for all of the five simulated species. The mean uncertainty reduction for CO_2 emissions from fossil fuels is roughly 38%, for GEE it is around 41% while for respiration it is roughly 44%. For CO and CH_4 the uncertainty reduction is about 63% and 67% respectively. Finally, we described quantitatively the benefit of using multi-species inversions by exploiting correlations in different chemical species. It is found that considering correlations between different trace gases can reduce the posterior uncertainty by up to about 20% for monthly fluxes. These benefits are however dependent on the error structure of the prior uncertainty.

The present paper paves the way for future studies using simultaneous measurements of different trace gases. This will be especially important in the context of the upcoming routine measurements of CO_2, CO, and CH_4 vertical profiles within IAGOS. As IAGOS makes use of commercial airliners, such profiles will be collected in the vicinity of major international airports, and hence in the vicinity of major metropolitan areas, where many different human activities take place simultaneously. In such a context, any improvement in the constraint of atmospheric inversions will be particularly useful. A possible improvement in this analysis would be to evaluate the effects of different correlation factors specific to different pairs of anthropogenic species, fuels and emission sectors.

5. Acknowledgements

The research leading to these results has received funding from the European Community's Seventh Framework Programme ([FP7/2007-2013]) under grant agreement n° 312311 (IGAS).
The authors acknowledge the strong support of the European Commission, Airbus, and the Airlines (Lufthansa, Air-France, Austrian, Air Namibia, Cathay Pacific, Iberia and China Airlines so far) who carry the MOZAIC or IAGOS equipment and perform the maintenance since 1994. In its last 10 years of operations MOZAIC has been funded by INSU-CNRS (France), Météo-France, Université Paul Sabatier (Toulouse, France) and Research Center Jülich (FZJ, Jülich, Germany). The IAGOS database is supported by AERIS (CNES and INSU-CNRS). Data are also available via AERIS web site http://www.aeris-data.fr

References

Berezin, E. V., Konovalov, I. B., Ciais, P., Broquet, G., Wu, L., Beekmann, M, Hadji-Lazaro, J., Clerbaux, C., Andreae, M. O., Kaiser, J. W., Schulze, E. D.: CO_2 emissions from wildfires in Siberia: FRP measurement based estimates constrained by satellite and ground based observations of co-emitted species. In Geophysical Research Abstracts (Vol. 15), 2013.

Bergamaschi, P., Hein, R., Heimann, M., Crutzen, P. J.: Inverse modeling of the global CO cycle: 1. Inversion of CO mixing ratios, J. Geophys. Res., 105(D2), 1909-1927, 2000.

Boschetti, F., Chen, H., Thouret, V., Nedelec, P., Janssens-Maenhout, G., Gerbig, C.: On the representation of IAGOS/MOZAIC vertical profiles in chemical transport models: contribution of different error sources in the example of carbon monoxide, Tellus B, 67, 2015.

Brioude, J., Angevine, W. M., Ahmadov, R., Kim, S. W., Evan, S., McKeen, S., Hsie, E. Y., Frost, G. J., Neuman, J. A., Pollack, I. B., Peischi, J.: Top-down estimate of surface flux in the Los Angeles Basin using a mesoscale inverse modeling technique: assessing anthropogenic emissions of CO, NOx and CO2 and their impacts, Atmos. Chem. Phys., 13(7), 3661-3677, 2013.

Brioude, J., Petron, G., Frost, G. J., Ahmadov, R., Angevine, W. M., Hsie, E. Y., Kim, S. W., Lee, S. H., McKeen, S. A., Trainer, M., Fehsenfeld, F. C., Holloway, J. S., Peischl, J., Ryerson, T. B. and Gurney, K. R.: A new inversion method to calculate emission inventories without a prior at mesoscale: Application to the anthropogenic CO 2emission from Houston, Texas, J. Geophys. Res., 117(D5), D05312, doi:10.1029/2011JD016918, 2012.

Bousquet, P., Ciais, P., Miller, J.B., Dlugokencky, E.J., Hauglustaine, D.A., Prigent, C., Van der Werf, G.R., Peylin, P., Brunke, E.G., Carouge, C. and Langenfelds, R.L.: Contribution of anthropogenic and natural sources to atmospheric methane variability, Nature, 443(7110), 439-443, 2006.

BP (British Petroleum), 2014. Statistical Review of World Energy: http: //www.bp.com/statisticalreview, last access: September 2014.

Cain, M., Warwick, N. J., Fisher, R. E., Lowry, D., Lanoisellé, M., Nisbet, E. G., France, J., Pitt, J., O'Shea, S., Bower, K. N., Allen, G., Illingworth, S., Manning, A. J., Bauguitte, S., Pisso, I. and Pyle, J. A.: A cautionary tale: A study of a methane enhancement over the North Sea, J Geophys Res-Atmos, 122(14), 7630–7645, doi:10.1038/s41598-017-04802-6, 2017.

Denier van der Gon, H. D., Hendriks, C., Kuenen, J., Segers, A., and Visschedijk, A.: Description of current temporal emission patterns and sensitivity of predicted AQ for temporal emission patterns, TNO Report, EU FP7 MACC deliverable report D_D- EMIS_1.3, available at: https://gmes-atmosphere.eu/documents/ deliverables/d-emis/MACC_TNO_del_1_3_v2.pdf, 2011.

European Commission, Joint Research Centre (JRC)/Netherlands Environmental Assessment Agency (PBL): Emission Database for Global Atmospheric Research (EDGAR), release version 4.1 and 4.2. http://edgar.jrc.ec.europa.eu, 2011.

FAO, Food and Agricultural Organization: FAO Statistical Yearbook 2013 – World food and agriculture, http://www.fao.org/docrep/018/i3107e/i3107e.PDF, 2013

Filges, A., Gerbig, C., Chen, H., Franke, H., Klaus, C. and Jordan, A.: The IAGOS-core greenhouse gas package: a measurement system for continuous airborne observations of CO 2, CH 4, H 2 O and CO, Tellus B, 67, 2015.

Friedlingstein, P., Cox, P., Betts, R., Bopp, L., Von Bloh, W., Brovkin, V., Cadule, P., Doney, S., Eby, M., Fung, I. and Bala, G.: Climate–carbon cycle feedback analysis: results from the C4MIP model intercomparison, Journal of Climate, 19(14), pp.3337-3353, 2006.

Gerbig, C., Lin, J. C., Wofsy, S. C., Daube, B. C., Andrews, A. E., Stephens, B. B., Bakwin, P. S. and Grainger, C. A.: Toward constraining regional-scale fluxes of CO2 with atmospheric observations over a continent: 2. Analysis of COBRA data using a receptor-oriented framework, J Geophys Res-Atmos, 108(D24), doi:10.1029/2003JD003770, 2003.

Gourdji, S.M.: North American CO2 exchange: Inter comparison of modeled estimates with results from a fine scale atmospheric inversion, Biogeosciences, 2013.

Heimann, M., and Körner, S.: The global atmospheric tracer model TM3. Technical Reports, Max-Planck-Institut für Biogeochemie, 5, pp.131, 2003.

Hein, R., Crutzen, P.J. and Heimann, M.: An inverse modeling approach to investigate the global atmospheric methane cycle, Global Biogeochemical Cycles, 11(1), 43-76, 1997.

IEA (International Energy Agency) World Energy Outlook 2014, http://www.iea.org/bookshop/720-World_Energy_Outlook_2014, 2014.

IPCC: Climate Change 2014: Synthesis Report. Contribution of Working Groups I, II, and III to the Fifth Assessment Report of the Intergovernmental Panel on Climate Change [Core Writing Team, R.K. Pachauri and L.A. Meyer (eds.)], IPCC, Geneva, Switzerland, 151 pp., 2014

Janssens-Maenhout, G., Pagliari, V., Guizzardi, D., Muntean, M.: Global emission inventories in the Emission Database for Global Atmospheric Research (EDGAR) – Manual (I): Gridding: EDGAR emissions distribution on global gridmaps. JRC Report, EUR 25785 EN, 2013.

Jung, M., Henkel, K., Herold, M. and Churkina, G.: Exploiting synergies of global land cover products for carbon cycle modeling, Remote Sensing of Environment, 101(4), 534-553, 2006.

Kadygrov, N., Broquet, G., Chevallier, F., Rivier, L., Gerbig, C. and Ciais, P.: On the potential of the ICOS atmospheric CO 2 measurement network for estimating the biogenic CO_2 budget of Europe. Atmos. Chem. Phys., 15(22), 12765-12787, 2015.

Christoph Gerbig 20.12.17 09:17
Gelöscht: CO 2

Karion, A., Sweeney, C., Kort, E. A., Shepson, P. B., Brewer, A., Cambaliza, M., Conley, S. A., Davis, K., Deng, A., Hardesty, M., Herndon, S. C., Lauvaux, T., Lavoie, T., Lyon, D., Newberger, T., Pétron, G., Rella, C., Smith, M., Wolter, S., Yacovitch, T. I. and Tans, P.: Aircraft-Based Estimate of Total Methane Emissions from the Barnett Shale Region, Environ. Sci. Technol., 49(13), 8124–8131, doi:10.1021/acs.est.5b00217, 2015.

Kort, E. A., Smith, M. L., Murray, L. T., Gvakharia, A., Brandt, A. R., Peischl, J., Reyerson, T. B., Sweeney, C., and Travis, K.: Fugitive emissions from the Bakken shale illustrate role of shale production in global ethane shift,1–7, doi:10.1002/2016GL068703, 2016.

Konovalov, I. B., Berezin, E. V., Ciais, P., Broquet, G., Beekmann, M., Hadji-Lazaro, J., Clerbaux, C., Andreae, M. O., Kaiser, J. W. and Schulze, E. D.: Constraining CO_2 emissions from open biomass burning by satellite observations of co-emitted species: a method and its application to wildfires in Siberia, Atmos. Chem. Phys., 14(19), 10383–10410, doi:10.5194/acp-14-10383-2014, 2014.

Kountouris, P., Gerbig, C., Rödenbeck, C., Karstens, U., Koch, T. F. and Heimann, M.: Atmospheric CO_2 inversions at the mesoscale using data driven prior uncertainties. Part2: the European terrestrial CO_2 fluxes, Atmos. Chem. Phys. Discuss., 1–44, doi:10.5194/acp-2016-578, 2016.

Lin, J. C. and Gerbig, C.: Accounting for the effect of transport errors on tracer inversions, Geophys. Res. Lett., 32(1), L01802, doi:10.1029/2004GL021127, 2005.

Lin, J., Gerbig, C., Wofsy, S., Andrews, A., Daube, B., Davis, K. and Grainger, C.: A near-field tool for simulating the upstream influence of atmospheric observations: The Stochastic Time-Inverted Lagrangian Transport (STILT) model, J. Geophys. Res., 108(D16), 4493, doi:10.1029/2002JD003161, 2003.

Lyon, D. R., Zavala-Araiza, D., Alvarez, R. A., Harriss, R., Palacios, V., Lan, X., Talbot, R., Lavoie, T., Shepson, P., Yacovitch, T. I., Herndon, S. C., Marchese, A. J., Zimmerle, D., Robinson, A. L. and Hamburg, S. P.: Constructing a Spatially Resolved Methane Emission Inventory for the Barnett Shale Region, Environ. Sci. Technol., 49(13), 8147–8157, doi:10.1021/es506359c, 2015.

Machida, T., Matsueda, H., Sawa, Y., Nakagawa, Y., Hirotani, K., Kondo, N., Goto, K., Nakazawa, T., Ishikawa, K. and Ogawa, T.: Worldwide Measurements of Atmospheric CO 2and Other Trace Gas Species Using Commercial Airlines, J. Atmos. Oceanic Technol., 25(10), 1744–1754, doi:10.1175/2008JTECHA1082.1, 2008.

Mahadevan, P., Wofsy, S. C., Matross, D. M., Xiao, X., Dunn, A. L., Lin, J. C.: A satellite-based biosphere parameterization for net ecosystem CO 2exchange: Vegetation Photosynthesis and Respiration Model (VPRM). Global Biogeochemical Cycles, 22(2), n/a–n/a. doi:10.1029/2006GB002735, 2008.

Marenco, A., Thouret, V., Nédélec, P., Smit, H., Helten, M., Kley, D., Karcher, F., Simon, P., Law, K. and Pyle, J.: Measurement of ozone and water vapor by Airbus in, J.le, J.le, J.le,The MOZAIC airborne program, An overview, Journal of Geophysical Research: Atmospheres, 103(D19), 25631–25642, 1998.

Palmer, P. I., Suntharalingam, P., Jones, D. B. A., Jacob, D. J., Streets, D. G., Fu, Q.: Using CO2:CO correlations to improve inverse analyses of carbon fluxes. Journal of Geophysical Research, 111(D12), D12318. doi:10.1029/2005JD006697, 2006.

Pandey, S., Houweling, S., Krol, M., Aben, I. and Röckmann, T.: On the use of satellite-derived CH_4 : CO_2 columns in a joint inversion of CH_4 and CO_2 fluxes, Atmos. Chem. Phys., 15(15), 8615–8629, doi:10.5194/acp-15-8615-2015, 2015.

Peischl, J., Ryerson, T. B., Brioude, J., Aikin, K. C., Andrews, A. E., Atlas, E., Blake, D., Daube, B. C., de Gouw, J. A., Dlugokencky, E., Frost, G. J., Gentner, D. R., Gilman, J. B., Goldstein, A. H., Harley, R. A., Holloway, J. S., Kofler, J., Kuster, W. C., Lang, P. M., Novelli, P. C., Santoni, G. W., Trainer, M., Wofsy, S. C. and Parrish, D. D.: Quantifying sources of methane using light alkanes in the Los Angeles basin, California, J Geophys Res-Atmos, 118(10), 4974–4990, doi:10.1002/jgrd.50413, 2013.

Petzold, A., Thouret, V., Gerbig, C., Zahn, A., Brenninkmeijer, C.A.M., Gallagher, M., Hermann, M., Pontaud, M., Ziereis, H., Boulanger, D., Nédélec, P., Smit, H.G.J., Cammas , J.-P., Volz-Thomas, A., and the IAGOS Team: Global-Scale Atmosphere Monitoring by In-Service Aircraft – Current Achievements and Future Prospects of the European Research Infrastructure IAGOS, Tellus B 67, 2015.

Pison, I., Bousquet, P., Chevallier, F., Szopa, S., and Hauglustaine, D.: Multi-species inversion of CH_4, CO and H_2 emissions from surface measurements. Atmospheric Chemistry and Physics, 9(14), 5281-5297, 2009

Prpich, G., Coulon, F. and Anthony, E. J.: Science of the Total Environment, Science of the Total Environment, The, 563-564(C), 731–740, doi:10.1016/j.scitotenv.2015.11.026, 2016.

Rödenbeck, C., Houweling, S., Gloor, M. and Heimann, M.: Time-dependent atmospheric CO2 inversions based on interannually varying tracer transport. Tellus B, 55(2), 488–497, 2003.

Christoph Gerbig 20.12.17 09:42

Gelöscht: Kountouris, P., Gerbig, C., Rödenbeck, C., Karstens, U., Koch, T. F. and Heimann, M.: Atmospheric CO_2 inversions at the mesoscale using data driven prior uncertainties. Part2: the European terrestrial CO_2 fluxes, Atmos. Chem. Phys. Discuss., 1–44, doi:10.5194/acp-2016-578, 2016. ... [3]

Rodgers, C. D.: Inverse Methods for Atmospheric Sounding: Theory and Practice, World Scientific Publishing Co. Pte. Ltd., Singapore, 238 pp., 2000.

Sawa, Y., Machida, T. and Matsueda, H., Aircraft observation of the seasonal variation in the transport of CO2 in the upper atmosphere. *Journal of Geophysical Research: Atmospheres*, *117*(D5), 2012.

Sasakawa, M., Shimoyama, K., Machida, T., Tsuda, N., Suto, H., Arshinov, M., Davydov, D., Fofonov, A., Krasnov, O., Saeki, T. and Koyama, Y.: Continuous measurements of methane from a tower network over Siberia.Tellus B, 62(5), pp.403-416, 2010.

Steinbach, J., Gerbig, C., Rödenbeck, C., Karstens, U., Minejima, C. and Mukai, H.: The CO2 release and Oxygen uptake from Fossil Fuel Emission Estimate (COFFEE) dataset: effects from varying oxidative ratios. Atmos. Chem. Phys., 11(14), 6855–6870, 2011.

Streets, D.G., Bond, T.C., Carmichael, G.R., Fernandes, S.D., Fu, Q., He, D., Klimont, Z., Nelson, S.M., Tsai, N.Y., Wang, M.Q. and Woo, J.H.: An inventory of gaseous and primary aerosol emissions in Asia in the year 2000, Journal of Geophysical Research: Atmospheres, 108(D21), 2003.

UNECE, United Nations Economic Commission for Europe, State of Europe's forests 2011 – Status and Trends in Sustainable Forest Management in Europe, http://www.unece.org/fileadmin/DAM/publications/timber/Forest_Europe_report_2011_web.pdf, 2011

Vardag, S. N., Gerbig, C., Janssens-Maenhout, G., and Levin, I.: Estimation of continuous anthropogenic CO_2: model-based evaluation of CO_2, CO, $\delta^{13}C(CO_2)$ and $\Delta^{14}C(CO_2)$ tracer methods, Atmos. Chem. Phys., 15,, doi:10.5194/acp-15-12705-2015, 2015.

Wang, H., Jacob, D.J., Kopacz, M., Jones, D.B.A., Suntharalingam, P., Fisher, J.A., Nassar, R., Pawson, S. and Nielsen, J.E.: Error correlation between CO 2 and CO as constraint for CO 2 flux inversions using satellite data, Atmospheric Chemistry and Physics, 9(19), pp.7313-7323, 2009.

Zbinden, R.M., Thouret, V., Ricaud, P., Carminati, F., Cammas, J.P. and Nédélec, P., Climatology of pure tropospheric profiles and column contents of ozone and carbon monoxide using MOZAIC in the mid-northern latitudes (24° N to 50° N) from 1994 to 2009. *Atmospheric Chemistry and Physics*, *13*(24), pp.12363-12388,2013.

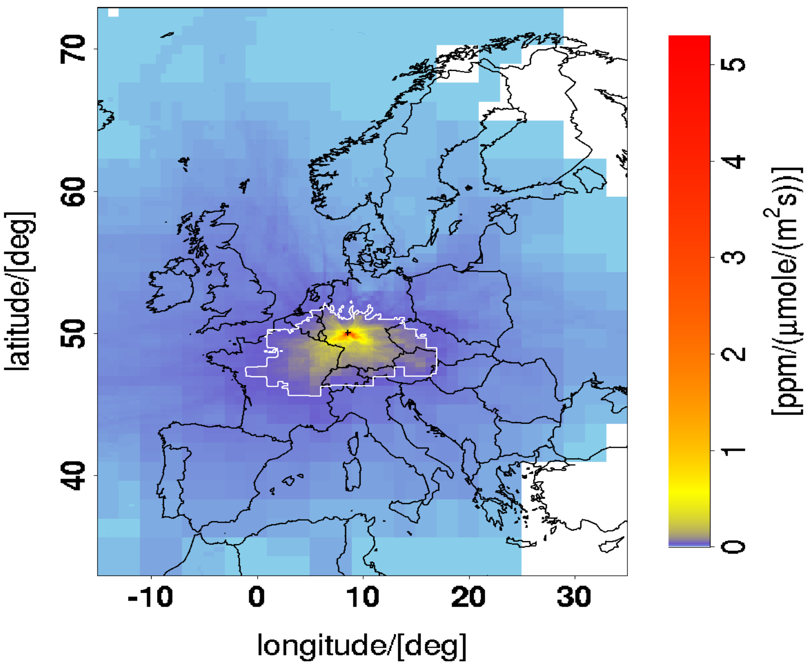

Figure 1: Cumulative sum of the ML footprints for all the flights into or out of FRA in the year 2011. The gray line delineates the 50% footprint.

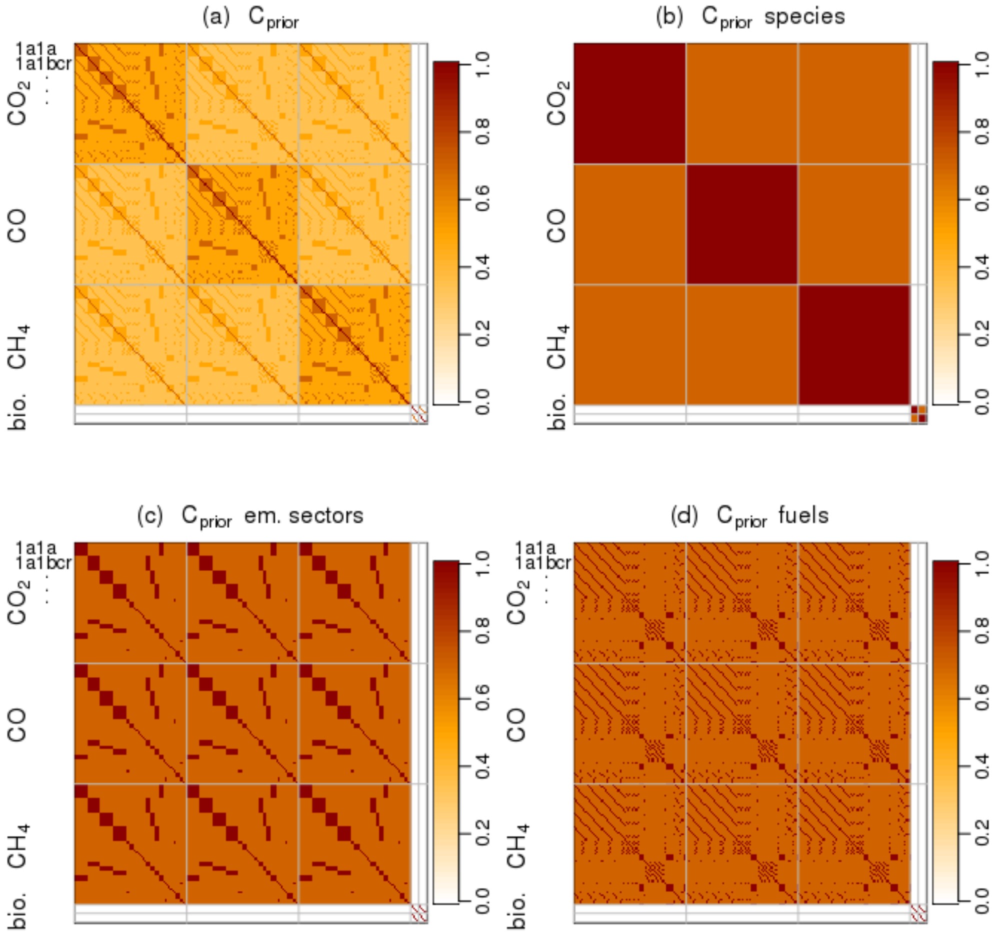

Figure 2: Prior error correlation matrix (a) used in the multi-species inversion, and the respective components for modeled species (b), emission sectors (c) and fuel types (d). Matrix (a) is the element-wise product of matrices (b), (c) and (d). Each matrix has the same dimensions (2604x2604) reflecting the length of the state vector. The matrices are shown for only one month here, for illustration. The gray lines indicates subsets of the flux categories according to different modeled species ('blocks'), ordered as follows from top to bottom and from left to right: anthropogenic CO_2, CO, CH_4, GEE and respiration. In the single-species inversion, the correlation values in the off-diagonal 'blocks' of matrix (b) are set to zero. In the complete matrix, correlation between fluxes from different months is also set to zero.

Christoph Gerbig 20.12.17 13:26

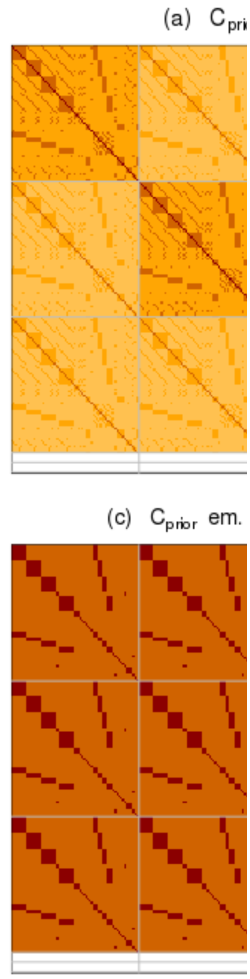

Gelöscht:

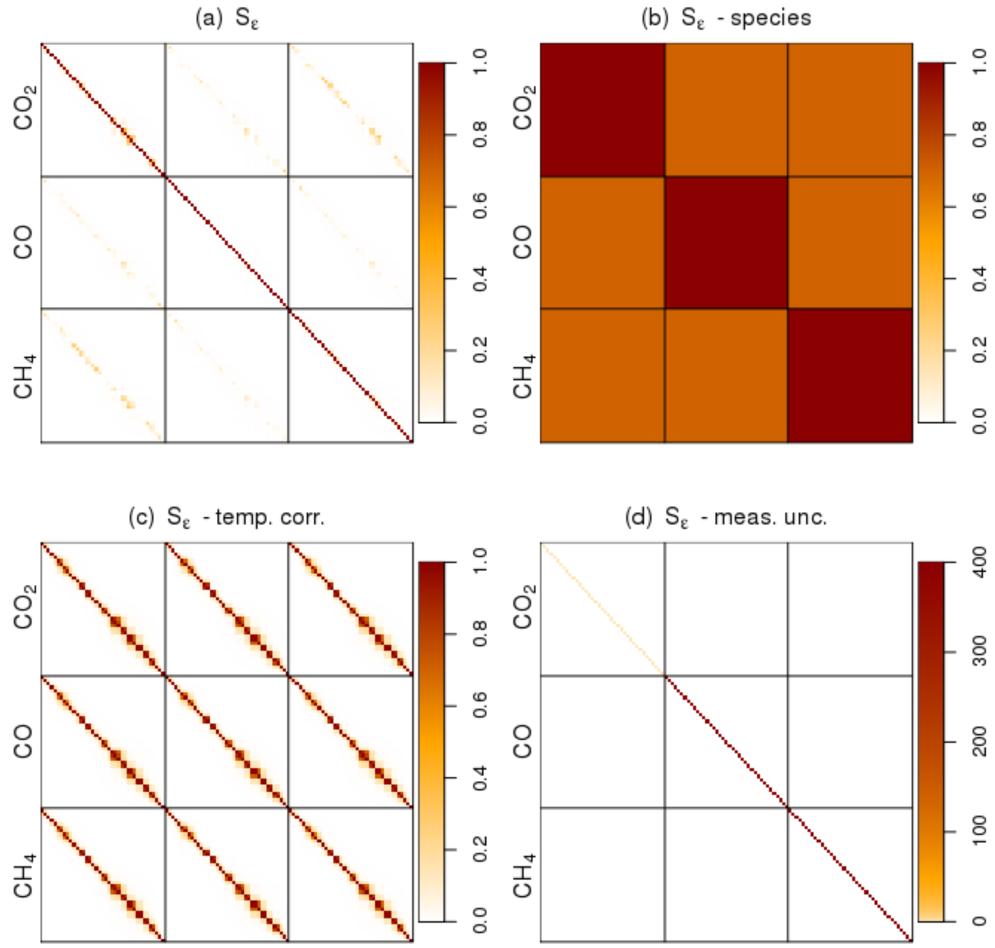

Figure 3: Model-data mismatch correlation matrix (a) used in the multi-species inversion, species correlation matrix S_s (b), temporal correlation matrix S_t (c) and squared measurement uncertainty (d). Note that the measurement uncertainty is expressed in ppm for CO_2 and ppb for CO and CH_4. Each matrix has the same dimensions (1098x1098) reflecting the length of the observation vector, but here only the data of July are plotted to increase visibility. The gray lines indicate different species in the observation vector ('blocks'), ordered as follows from top to bottom and from left to right: total CO_2, CO and CH_4. In the single-species inversion, the correlation value in the off-diagonal 'blocks' of matrix (b) is set to zero. The structure in S_s in (c) is a result of the uneven temporal distribution of the observations within the month.

Christoph Gerbig 20.12.17 13:31

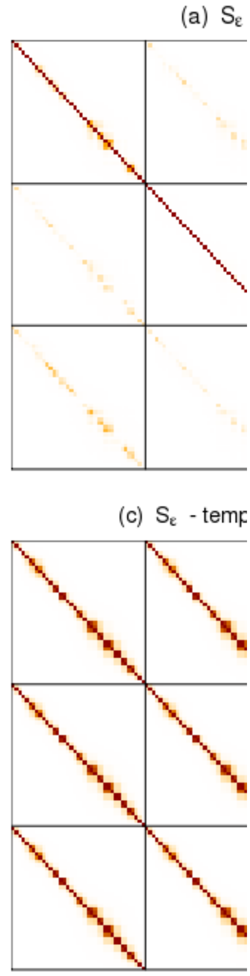

Gelöscht:

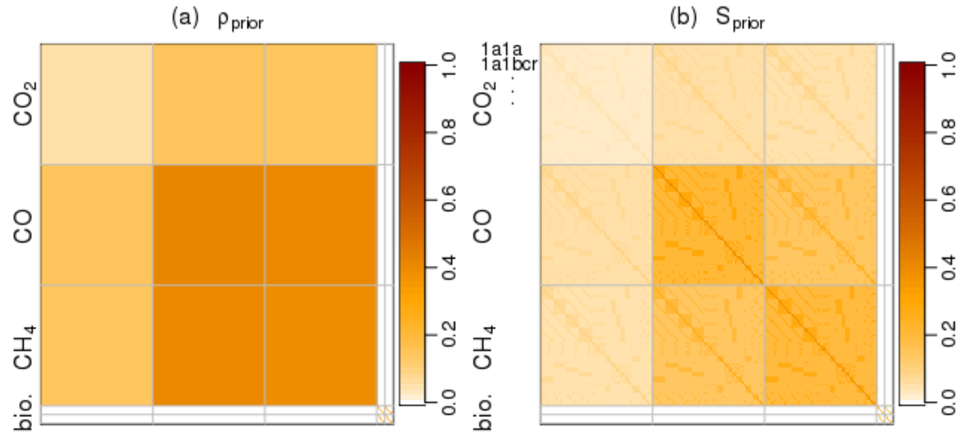

Figure 4: The final rescaling matrix ρ_{prior} (a) and the prior error covariance matrix S_{prior}(b). Note that ρ_{prior} can be defined as the element-wise ratio of S_{prior} and C_{prior}.

Christoph Gerbig 20.12.17 13:34

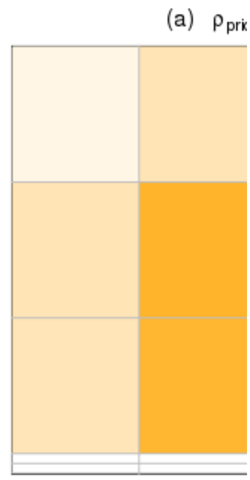

Gelöscht:

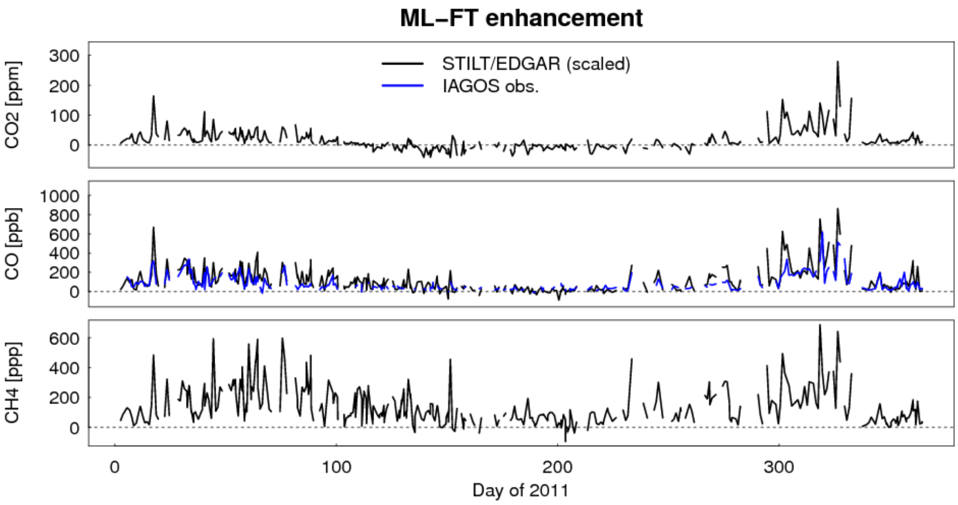

Figure 5: Mean daily enhancement of mixed layer vs. free tropospheric mole fractions. Modeled mixing ratios are shown as black lines, while the observed CO is shown as blue line. Note that the modeled values for CO have been multiplied by a factor of 2.8, corresponding to the mean ratio between observed and modeled CO enhancements, to match the observed values.

Christoph Gerbig 18.12.17 16:05

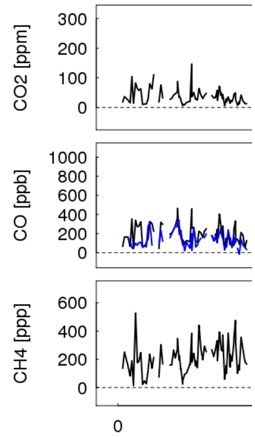

Gelöscht:

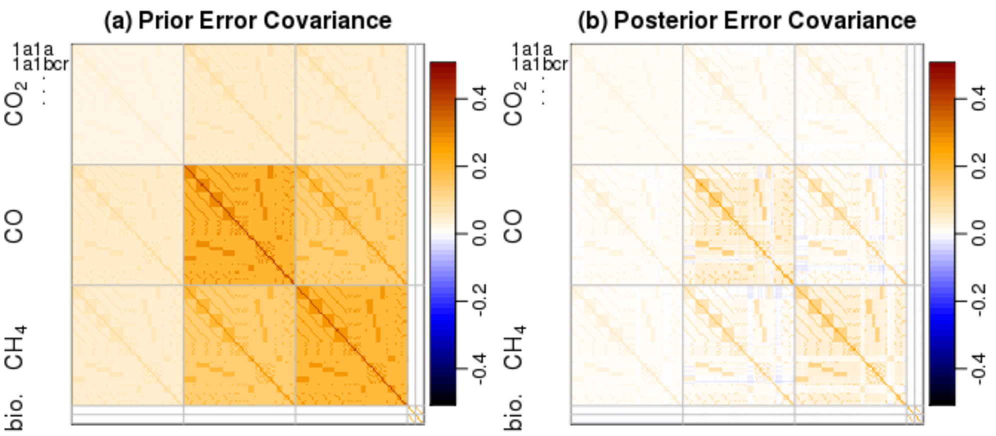

Figure 6: Prior error covariance matrix (left) and corresponding posterior error covariance matrix (right).

Christoph Gerbig 20.12.17 13:37

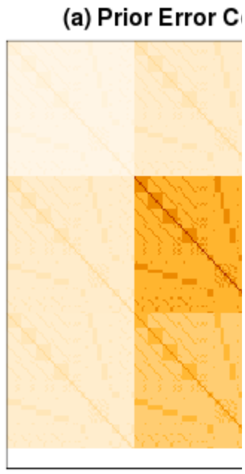

Gelöscht:

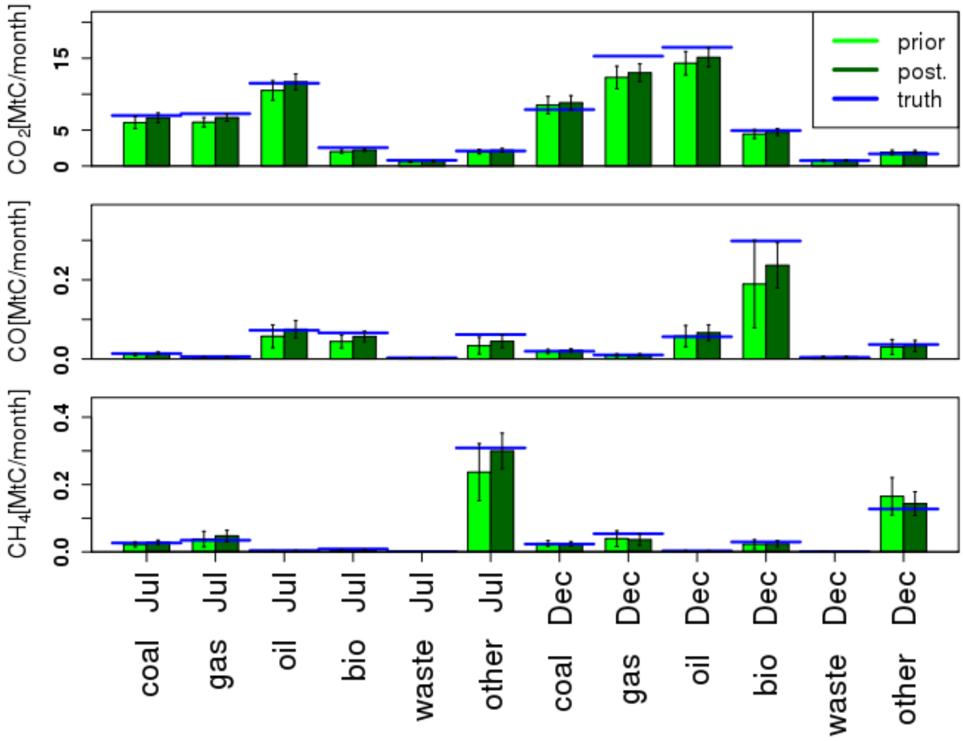

Figure 7: Prior, posterior and true (pseudo-data) fluxes in physical units aggregated for different fuel types. Note that, as the true fluxes are the result of a random perturbation of the prior, they do not describe an actual situation in the physical world. So, for example, the fact that the true value of CH_4 fluxes in July is lower than the same value in December should not be surprising.

Christoph Gerbig 21.12.17 09:37

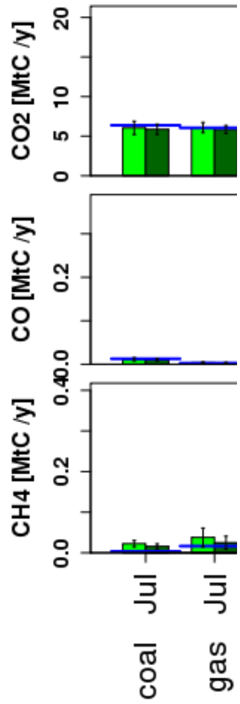

Gelöscht:

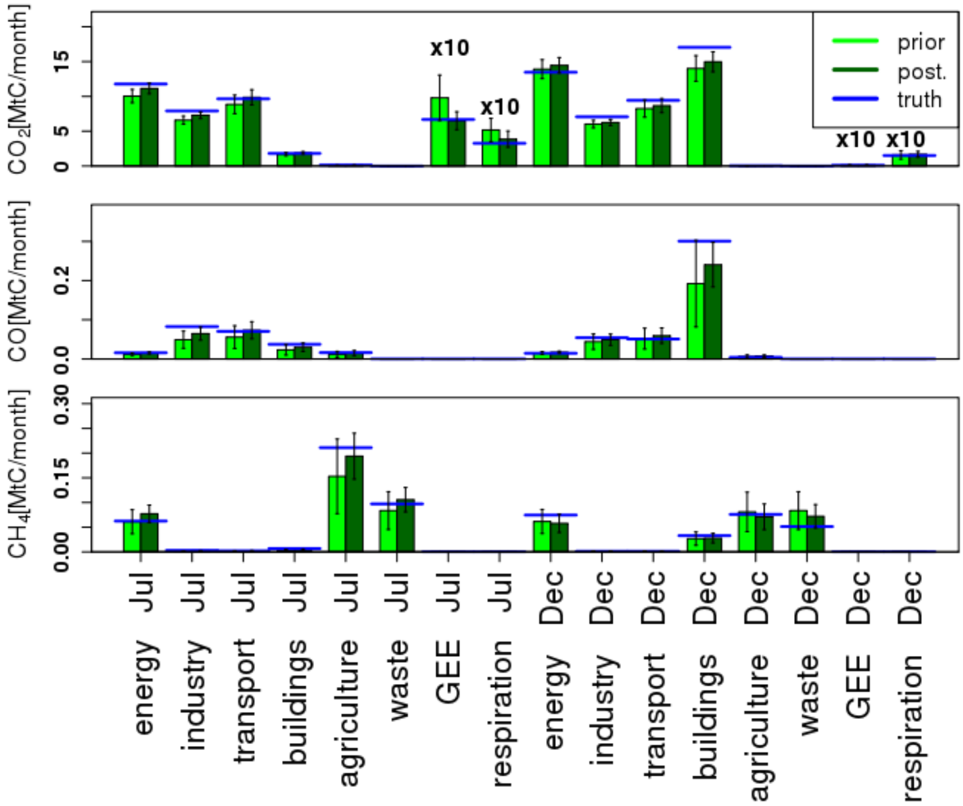

Figure 8: Prior, posterior and true (pseudo-data) fluxes in physical units aggregated for different emission sectors. Absolute values of biosphere-atmosphere exchange fluxes of CO_2 are included in (b), but scaled down by a factor of 10. Note that, as the true fluxes are the result of a random perturbation of the prior, they do not describe an actual situation in the physical world. So, for example, the fact that the true value of CO for transport in July is higher than the same value in December should not be surprising.

Christoph Gerbig 21.12.17 09:38

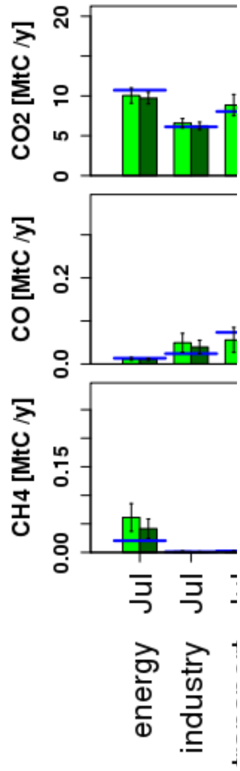

Gelöscht:

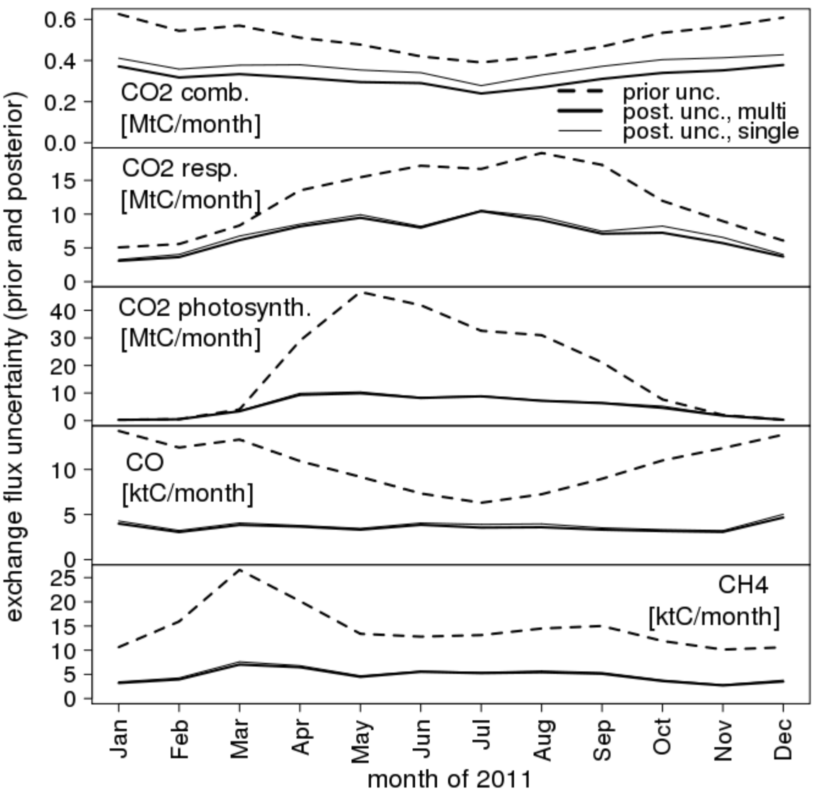

Figure 9: Comparison between prior and posterior monthly uncertainties for the five tracers. The posterior uncertainty is plotted for both the multi-species inversion, accounting for inter-species correlations, and the single-species inversion, in which all of the species are independent. Both prior and posterior uncertainty are expressed in physical units. The spike in the prior methane uncertainty estimate for the month of March depends on the emission inventory and is related to the cycle of agricultural activities.

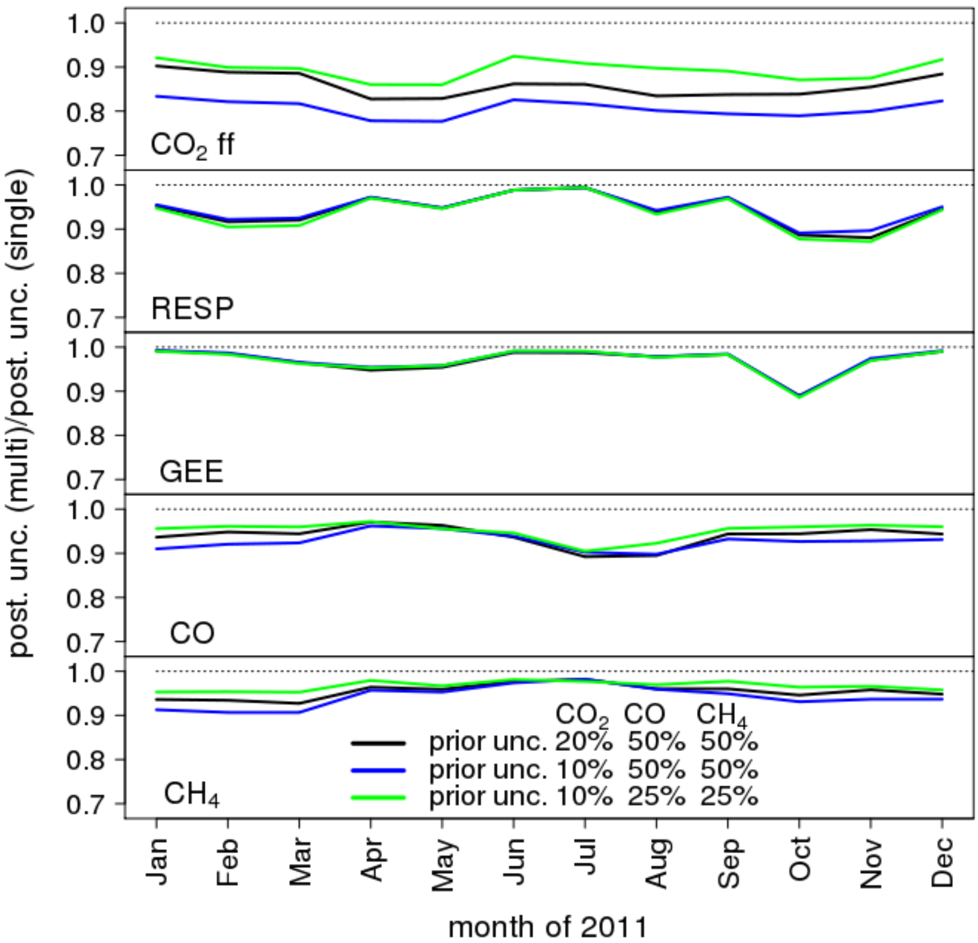

Christoph Gerbig 21.12.17 09:43

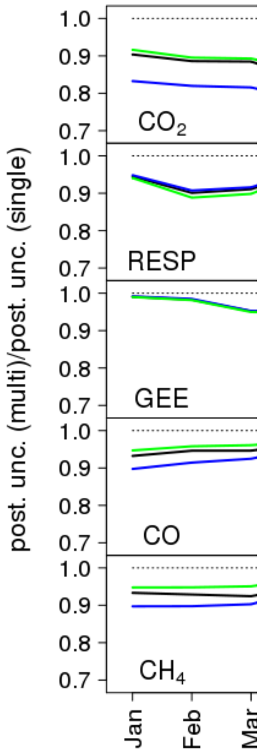

Gelöscht:

Figure 10: Benefit of a multi-species inversion over the corresponding single-species (dotted line) per different species per months of the year. The benefit has been tested for the three different cases of Table 3. Note that CO_2 refers to fossil fuel emissions only, and RESP and GEE refers to the biospheric fluxes.

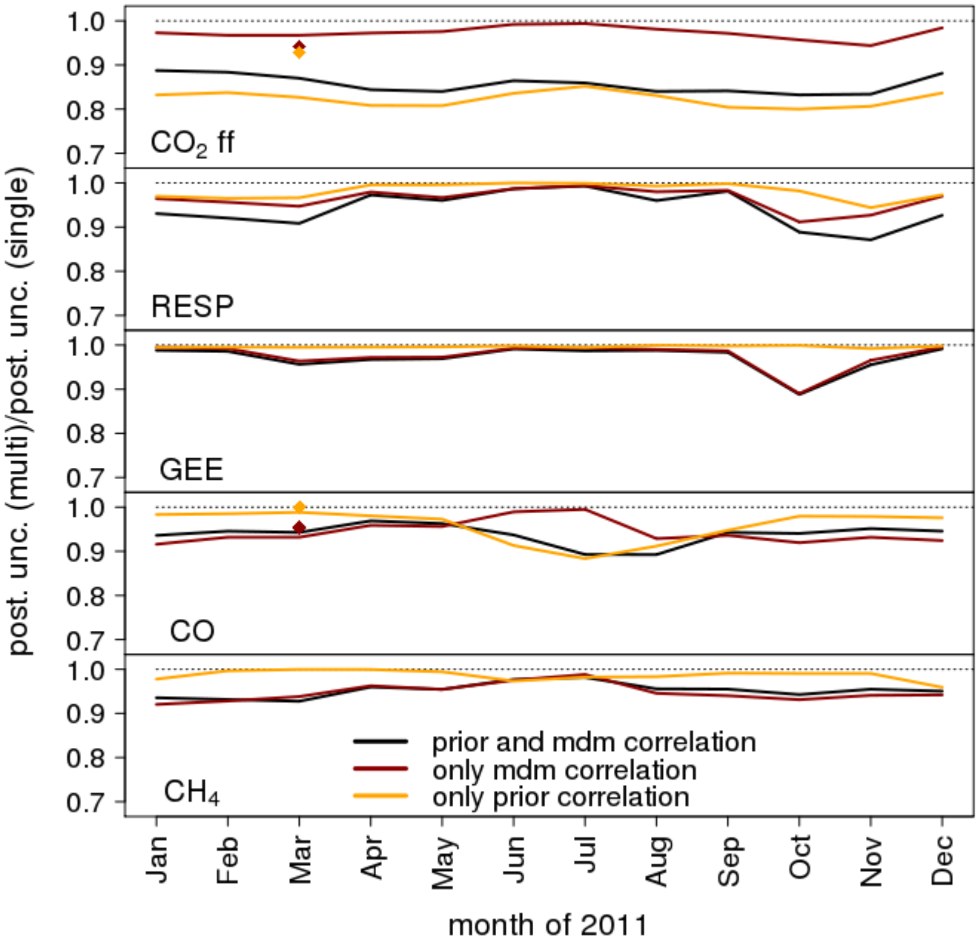

Christoph Gerbig 21.12.17 09:57

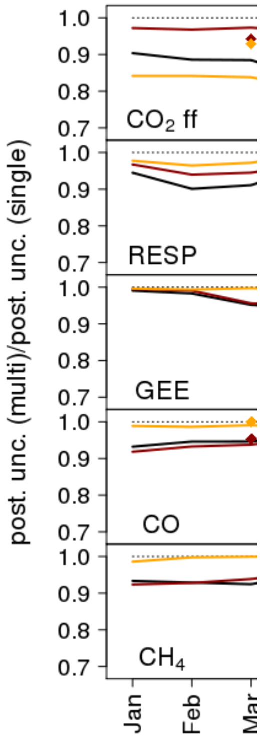

Gelöscht:

Figure 11: Benefit of a multi-species inversion over the corresponding single-species (dotted line) per different species and month. The benefit has been tested for a "normal" inversion featuring both prior and model-data mismatch correlation between different species (black) or only one of these two components (red and orange). Results refer to Case 1 of Table 3 (black line of Fig. 10). Values derived from Palmer (2006) for the month of March are indicated with a diamond.

	Adj IPCC	Description	Aggregated
1	1a1a	Power generation	Energy
2	1a1bcr	Other transformation non-energy use	Energy
3	1b1	Solid fuels production	Energy
4	1b2abc	Gas flaring	Energy
5	1b2ac	Oil prod., distribution and flaring	Energy
6	1b2b	Gas production and distribution	Energy
7	1a3a+1c1	International and domestic aviation	Transport
8	1a3b	Road transport	Transport
9	1a3ce	Non-road ground transport	Transport
10	1a3d+1c2	Inland waterways and shipping	Transport
11	1a2+6cd	Industrial combustion (non-power)	Industry
12	2a	Cement and lime production	Industry
13	2befg+3	Chemical industry and solvent	Industry
14	2c	Metal industry emission	Industry
15	1a4	Buildings	Buildings
16	4a	Enteric fermentation in agriculture	Agriculture
17	4b	Manure management	Agriculture
18	4c	Rice cultivation	Agriculture
19	4f	Agricultural waste burning	Agriculture
20	6a	Solid waste disposal in landfills	Waste
21	6b	Wastewater treatment	Waste
22	7a	Fossil fuel fires	FF_fuels

Table 1: Specific emission sectors accounted for in the state vector and aggregated categories as used in Fig. 8.

	Fuel type	Aggregated fuel type
1	Brown coal	Coal
2	Hard coal	Coal
3	Peat	Coal
4	Gas derivatives	Gas
5	Natural gas	Gas
6	Heavy oil	Oil
7	Light oil	Oil
8	Solid waste	Waste
9	Venting and flaring	Oil
10	Other (*)	Other
11	Gas biofuels	Bio
12	Liquid biofuels	Bio
13	Solid biofuels	Bio

Table 2: Specific fuel types accounted for in the state vector and aggregated categories as used in Fig. 8.
(*) The category "Other" is derived by summing the contribution from those processes in which is difficult to establish the specific fuel responsible for the emissions.

	CO_2	CO	CH_4
Case 1	20%	50%	50%
Case 2	10%	50%	50%
Case 3	10%	25%	25%

Table 3: relative uncertainty of the prior fluxes aggregated domain-wide and annual for the different cases

	Prior - Truth ($MtC\ y^{-1}$)	Posterior - Truth ($MtC\ y^{-1}$)	Pert. Prior - Truth ($MtC\ y^{-1}$)
CO_2 ff	-14.2	1.5 (-111 %)	-8.8 (-38 %)
CO	-0.95	-0.29 (-69 %)	-1.08 (+13 %)
CH_4	0.36	0.11 (-68 %)	0.84 (+133 %)
GEE	-81.8	-17.9 (-78 %)	-116.8 (+43 %)
Respiration	39.5	20.6 (-48 %)	62.2 (+58 %)

Table 4: Overall bias for different species between the prior and both posterior and perturbed prior. The percentage values in parenthesis refer to the corresponding Prior-Truth bias.

Christoph Gerbig 9.1.18 17:37
Gelöscht: 79.2
Christoph Gerbig 18.12.17 16:05
Gelöscht: 67.5 (-15
Christoph Gerbig 9.1.18 17:48
Gelöscht: 104.1…8.8 (-+31 ... [4]
Christoph Gerbig 9.1.18 17:37
Gelöscht: 1.3
Christoph Gerbig 9.1.18 17:39
Gelöscht: 1.0…0.29 (-28 ... [5]
Christoph Gerbig 9.1.18 17:48
Gelöscht: 1.9…1.08 (+42 ... [6]
Christoph Gerbig 9.1.18 17:38
Gelöscht: 2.2
Christoph Gerbig 9.1.18 17:39
Gelöscht: 1.….11 (-680 (-52 ... [7]
Christoph Gerbig 9.1.18 17:48
Gelöscht: 3.0….84 (+37 ... [8]
Christoph Gerbig 9.1.18 17:38
Gelöscht: 184.1
Christoph Gerbig 9.1.18 17:39
Gelöscht: 79.3…17.9 (-57 ... [9]
Christoph Gerbig 9.1.18 17:48
Gelöscht: 373.1…116.8 (+102 ... [10]
Christoph Gerbig 9.1.18 17:38
Gelöscht: 151.4
Christoph Gerbig 18.12.17 16:05
Gelöscht: 91.2 (-40
Christoph Gerbig 9.1.18 17:49
Gelöscht: 221….2.22… (+46 ... [11]

Correlation	Post-Truth CO_2 ff	Post-Truth CO	Post-Truth CH_4	Post-Truth GEE	Post-Truth Respiration
0.1	-6.3 ±16.4	-0.3 ± 0.2	-0.1 ± 0.3	-18.5 ± 23.6	-19.0 ±27.5
0.2	-4-4 ±16.1	-0.3 ± 0.2	0.0 ± 0.3	-18.6 ± 23.5	-19.2 ±27.4
0.3	-2.7 ±15.9	-0.3 ± 0.2	0.0 ± 0.3	-18.6 ± 23.4	-19.5 ±27.3
0.4	-1.3 ±15.6	-0.3 ± 0.2	0.0 ± 0.3	-18.5 ± 23.4	-19.7 ±27.3
0.5	-0.1 ± 15.2	-0.3 ± 0.2	0.0 ± 0.2	-18.4 ± 23.3	-20.0 ±27.2
0.6	0.8 ± 14.6	0.3 ± 0.2	0.1 ± 0.2	-18.2 ± 23.2	-20.3 ±27.1
0.7	1.5 ± 13.7	-0.3 ± 0.2	0.1 ± 0.2	-17.9 ± 23.2	-20.6 ±26.9
0.8	1.9 ± 12.4	-0.3 ± 0.2	0.2 ± 0.2	-17.6 ± 23.1	-20.9 ±26.8
0.9	1.5 ± 10.4	-0.4 ± 0.2	0.3 ± 0.2	-17.3 ± 23.0	-21.1 ±26.5

Table 5: Residuals between total annual posterior fluxes and total annual true fluxes for the five simulated species (in MtC y^{-1}) and different inter-species correlation values in the prior error covariance matrix (first column). The corresponding posterior uncertainty was added for each Post-Truth value.

Christoph Gerbig 19.12.17 08:45
Formatiert: Schriftart:Fett

Christoph Gerbig 8.1.18 13:20
Formatiert: Hochgestellt

Christoph Gerbig 19.12.17 08:45
Formatiert: Schriftart:Fett

Seite 17: [1] Gelöscht	Christoph Gerbig	19.12.17 10:15

Dominant fuels for CO_2 are coal, gas and oil, whose prior fluxes (pseudo data) have a magnitude of 6-11 Megatons of carbon per year (MtC y^{-1}) in July and 8-14 MtC y^{-1} in December, while CO is dominated by a 0.19 MtC y^{-1} flux from biofuels during winter and secondary contributions during summer from oil and biofuels with a magnitude of 0.06-0.08 MtC y^{-1}. Regarding CH_4, the single dominant contribution is from "Other" fuels, responsible for 0.16-0.24 MtC y^{-1} of emissions. "Other" fuel types include emissions from non-metallic minerals industry (e.g. cement, lime), agricultural waste burning, metal industry processing, chemical and solvent industry, solid waste disposal in landfills, wastewater treatment, manure management in agriculture, rice cultivation in agriculture, and agricultural soil emissions. For CO_2, the dominant contribution from these "Other" fuels in the European domain is from the non-metallic mineral industry (1.13 MtC y^{-1}); for CO and CH_4, the lion's share of the "Other" fuels emission is from the metal industry (0.03 MtC y^{-1}) and agricultural waste burning (0.06-0.11 MtC y^{-1}).

The most important emission sectors for CO_2 are energy, industry, transport and building, each contributing 7-10 MtC y^{-1} in July and 6-14 MtC y^{-1} in December, while CO is dominated by a 0.19 MtC y^{-1} flux from buildings during winter with secondary contributions from industry and transport with a magnitude of 0.04 MtC y^{-1} and 0.05 MtC y^{-1} respectively in both the analyzed months. CH_4 is dominated by a contribution of 0.15 MtC y^{-1} flux from agriculture in July with secondary contributions from waste and energy with a magnitude of roughly 0.06-0.08 MtC y^{-1} in both July and December. The contribution from biospheric primary production is about 100 MtC y^{-1} in July, which drops to almost zero in December, while respiration values are 50 MtC y^{-1} in July and roughly 150 MtC y^{-1} in December.

Seite 17: [2] Gelöscht	Christoph Gerbig	18.12.17 16:05

To do so we calculated for each simulated species the overall bias for the whole year between the prior and both posterior and the perturbed prior

Seite 26: [3] Gelöscht	Christoph Gerbig	20.12.17 09:42

Kountouris, P., Gerbig, C., Rödenbeck, C., Karstens, U., Koch, T. F. and Heimann, M.: Atmospheric CO_2 inversions at the mesoscale using data driven prior uncertainties. Part2: the European terrestrial CO_2 fluxes, Atmos. Chem. Phys. Discuss., 1–44, doi:10.5194/acp-2016-578, 2016.

Seite 43: [4] Gelöscht	Christoph Gerbig	09.01.18 17:48

104.1

Seite 43: [4] Gelöscht	Christoph Gerbig	09.01.18 17:48

104.1

Seite 43: [5] Gelöscht	Christoph Gerbig	09.01.18 17:39

1.0

Seite 43: [5] Gelöscht	Christoph Gerbig	09.01.18 17:39

1.0

Seite 43: [6] Gelöscht	Christoph Gerbig	09.01.18 17:48

1.9

Seite 43: [6] Gelöscht	**Christoph Gerbig**	**09.01.18 17:48**

1.9

Seite 43: [7] Gelöscht	**Christoph Gerbig**	**09.01.18 17:39**

1.

Seite 43: [7] Gelöscht	**Christoph Gerbig**	**09.01.18 17:39**

1.

Seite 43: [8] Gelöscht	**Christoph Gerbig**	**09.01.18 17:48**

3.0

Seite 43: [8] Gelöscht	**Christoph Gerbig**	**09.01.18 17:48**

3.0

Seite 43: [9] Gelöscht	**Christoph Gerbig**	**09.01.18 17:39**

79.3

Seite 43: [9] Gelöscht	**Christoph Gerbig**	**09.01.18 17:39**

79.3

Seite 43: [10] Gelöscht	**Christoph Gerbig**	**09.01.18 17:48**

373.1

Seite 43: [10] Gelöscht	**Christoph Gerbig**	**09.01.18 17:48**

373.1

Seite 43: [11] Gelöscht	**Christoph Gerbig**	**09.01.18 17:49**

221.

Seite 43: [11] Gelöscht	**Christoph Gerbig**	**09.01.18 17:49**

221.

Seite 43: [11] Gelöscht	**Christoph Gerbig**	**09.01.18 17:49**

221.